

Ultrasound in Medicine & Biology

Towards fluoro-free interventions: Using radial intracardiac ultrasound for vascular navigation

--Manuscript Draft--

Manuscript Number:	UMB-D-21-00618R1
Article Type:	Original Contribution
Keywords:	Transcatheter interventions; Vascular navigation; Fluoro-free; Transfemoral guidance; Vascular Disease; Intracardiac echocardiography
Corresponding Author:	Hareem Nisar Western University London, ON CANADA
First Author:	Hareem Nisar
Order of Authors:	Hareem Nisar Leah Groves Leandro Cardarelli-Leite Terry M. Peters Elvis C.S. Chen
Abstract:	Transcatheter cardio-vascular interventions have the advantage of patient safety, reduced surgery time, and minimal trauma to the patient's body. Transcathether interventions, which are performed percutaneously, suffer from the lack of direct line-of-sight with the surgical tools and the patient anatomy. Therefore, such interventional procedures rely heavily on image guidance for navigating towards and delivering therapy at the target site. Vascular navigation via the inferior vena cava (IVC), from the groin to the heart, is an imperative part of most transcatheter cardiovascular interventions such as valve repair surgeries and ablation therapy. Traditionally, the IVC is navigated using fluoroscopic techniques such as angiography or CT venography. These X-ray based techniques can have detrimental effects on the patient as well as the surgical team, causing increased radiation exposure, increased risk of cancer, fetal defects, eye cataracts. The use of heavy lead apron has also been reported to cause back pain and spine issues thus leading to interventionalist's disc disease. We propose the use of a catheter-based ultrasound augmented with electromagnetic (EM) tracking technology to generate a vascular roadmap in real-time and perform navigation without harmful radiation. In this pilot study, we use intracardiac echocardiography (ICE) and tracking technology to reconstruct a vessel from a phantom in a 3D virtual space. This paper presents a pilot phantom study on ICE-based vessel reconstruction and demonstrates how the proposed ultrasound-based navigation will appear in a virtual space, by navigating a tracked guidewire within the vessels in the phantom without any radiation-based imaging. The geometric accuracy is assessed using a CT scan of the phantom, with a Dice coefficient of 0.79. The average distance between the surface of the two models comes out to be $1.7 \pm 1.12\text{mm}$.
Suggested Reviewers:	
Opposed Reviewers:	

To,
Christy K. Holland
Editor-in-Chief,
Ultrasound in Medicine and Biology (UMB)

Date: 20th August 2021

Subject: Cover Letter for UMB submission – “Towards fluoro-free interventions: Using radial intracardiac ultrasound for vascular navigation”

Dear Dr. Holland,

We are pleased to submit our research to the UMB journal. We state that this manuscript is of original contribution and has not and will not be submitted elsewhere for publication. The contribution from individual authors is stated as the following:

1. Hareem Nisar – primary researcher – design and execution of the study, performing all the experiments, most of the code generation, and writing the journal article.
2. Leah Groves – secondary researcher – part of the code generation, writing part of the paper, and editing the manuscript.
3. Leandro Cardarelli-Leite – clinical advisor – providing clinical motivation and regular insights towards the project, paper design, and editing.
4. Terry M. Peters – senior advisor – project supervision, grant holder, paper design and editing
5. Elvis C.S. Chen – senior advisor – project supervision, resource management, paper design, and editing.

All authors have individually approved the submission of this manuscript to UMB. Thank you for considering our submission.

In case of any query, please reach out to us at hnisar3@uwo.ca or chene@robarts.ca.

Best regards,

Hareem Nisar



Response to reviewers' comments

Title: *A simple, realistic walled phantom for intravascular and intracardiac applications*

Thank you for reviewing the paper and for providing us with valuable insights. We have incorporated your suggestions into the paper, mostly in the Discussion section. Additions to the original manuscript are centered and colored. The changes are also highlighted in the manuscript (attached as supplementary material). The changes have been made based on the expertise of the authors including a clinician.

Answers to Reviewer 1

Comment R1.1 *In clinical practice some intervention procedures need to be performed very quickly. Can the time used for vessel reconstruction be one of the limitations for clinical implication?*

Answer to R1.1 Thank you for pointing that out. Time consideration for the proposed workflow have been added to the 'Discussion' section of the paper on page no. 16-17, line no. 326-337 which says:

The phantom based workflow presented in this paper is time consuming due to the computationally expensive vessel segmentation technique used. For clinical purposes, the vessel segmentation step should be fast and robust. However, this is a first proof of concept study and the vessel segmentation step is only suitable for the phantom images. Therefore, to replace the current vessel segmentation step, we have developed a real-time segmentation technique for isolating vessel lumina from ultrasound imaging of inferior vena cava in animals.^a. We are also currently working towards optimizing the presented pipeline to perform the vessel reconstruction in order of seconds. Combining the optimized reconstruction algorithm with the real-time vessel segmentation method will enable a time-apt image guidance system ready for pre-clinical studies.

^aThe preprint has been made available at research gate (DOI: 10.13140/RG.2.2.31644.82567)

Comment R1.2 *The 3d reconstruction presented in Figure 4 focused only on 3D vessel reconstruction. In ultrasound-guided intervention we are used to define specific landmarks from the surrounding, which making orientation easier. Is this applicable in presented technology?*

Answer to R1.2 Yes, it would be possible to identify other landmarks based on where the operator is navigating. Since this is a radial ultrasound, the operator would be able to identify other anatomical landmarks forward to the probe tip, as well as lateral to the vessel. These features facilitate navigation.

Comment R1.3 *The phantom represents very ideal patients. Can artefacts from the surroundings (calcification, artificial material of implants..) affect the accuracy of your method?*

Answer to R1.3 The current pipeline is susceptible to errors when there are artifacts in the image. However, it will be mitigated in our future work. An explanation has been added in the 'Discussion' section of the paper on page no. 17, line no. 338-356 which states:

The accuracy of the vessel reconstruction algorithm presented in this paper largely depends on the accuracy of the vessel segmentation and the tracking technology used. The electromagnetic tracking has submillimeter accuracy, however the vessel segmentation does not. As mentioned earlier, we have developed a real-time vessel segmentation method using deep learning. This new segmentation method relies on a trained U-net model to accurately segment the complex-shaped vessel lumina from the ICE imaging of the vena cava from a swine. This deep learning based method is robust against boundary artifacts such as intraluminal buildups and stents. However, the algorithm produce inaccurate segmentation when a lead is present inside the vessel. Any artifacts outside the vessel and present in the surrounding tissue do not have a significant impact on the accuracy of our vessel segmentation and reconstruction. To cater for the any artefacts, the new segmentation technique can be trivially modified without disturbing the entire reconstruction pipeline presented in this paper. Deep learning based systems benefit from a variety of imaging datasets in making the segmentation algorithm more robust. By retraining the U-net model on different examples of vascular imaging with artifacts, the segmentation and thus the reconstruction can be made robust and accurate.

An example of successful and failed segmentation using our newly developed segmentation algorithm is shown in the figure below. Due to the lack of imaging dataset with artifacts, we augmented an ICE image of a swine vena cava with US reflections from a stent and lead. The top part of the figure shows that the algorithm successfully segments the vessel in the presence of a stent. The bottom half shows the inaccurate segmentation when a lead is present inside the vessel.

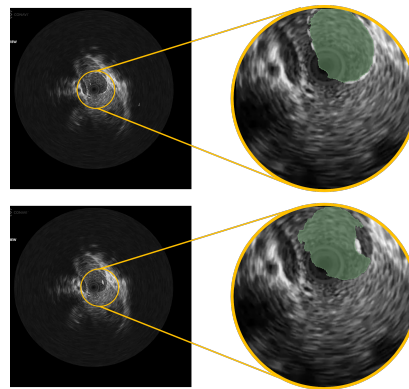


Figure R1: Qualitative evaluation of our deep-learning based segmentation algorithm when a stent (top) or a lead (bottom) is present within an ICE image.

Answers to Reviewer 2

Comment R2.1 *The US probe is limited technically in ability to guide into any branch vessels off the IVC making its clinical use unlikely as often interventionalist do not require fluoroscopy for advancement of wires and devices through the IVC. The study could be further strengthened by demonstrating ability to address this major limitation.*

Answer to R2.1 Thank you for your comments. The US probe is limited in its mobility because of the positioning of the tracking sensor in our experimental setup. In this preliminary study, We are using an existing Foresight ICE probe, already in the market. The Foresight ICE probe is now superceded by a much thinner and high frequency IVUS-OCT probe.

An explanation to address this limitation has been added in the 'Discussion' section of the paper on page no. 14-15, line no. 283-288, which states:

This limitation is strictly a characteristic of our experimental setup in this preliminary study using a Foresight™ ICE probe. The proposed idea can be extended to other radial ultrasound catheters as well. Ideally the tracking sensor should be integrated within the US catheter and pre-calibrated by the manufacturers to eliminate any limitation of maneuvering the US probe into the side vessels.

Comment R2.2 *Furthermore, authors do not compare the impact on procedure time using their model.*

Answer to R2.2 Time consideration for the proposed workflow have been added to the 'Discussion' section of the paper on page no. 16-17, line no. 326-337 which says:

The phantom based workflow presented in this paper is time consuming due to the computationally expensive vessel segmentation technique used. For clinical purposes, the vessel segmentation step should be fast and robust. However, this is a first proof of concept study and the vessel segmentation step is only suitable for the phantom images. Therefore, to replace the current vessel segmentation step, we have developed a real-time segmentation technique for isolating vessel lumina from ultrasound imaging of inferior vena cava in animals.^a. We are also currently working towards optimizing the presented pipeline to perform the vessel reconstruction in order of seconds. Combining the optimized reconstruction algorithm with the real-time vessel segmentation method will enable a time-apt image guidance system ready for pre-clinical studies.

^aThe preprint has been made available at research gate (DOI: 10.13140/RG.2.2.31644.82567)

Comment R2.3 *The ultrasound probe in this study is very large at 10 Fr, which significantly increases risk of vascular complications, it would be great to have authors address this and potential to miniaturize.*

Answer to R2.3 We agree that a 10 Fr device is quite big for the arterial system, although usually not an issue for venous interventions. This limitation has been addressed in the 'Discussion' section of the paper on page no. 17-18, line no. 357-366 which states:

Another limitation is the size of the US catheter. The US probe used in this study is a 10 Fr device which is large and less suitable for the arterial system, although it is usually not problematic for venous interventions. This is a limitation of the current technology (Foresight™ ICE probe by Conavi Medical Inc.) and ideally this device will be miniaturized by the manufacturers in the near future. The workflow presented in this paper can potentially be adapted for intravascular ultrasound (IVUS) imaging where the catheter is much smaller. For example, the Novasight Hybrid (by Conavi Medical Inc.) is a combined IVUS-OCT imaging catheter with a size of 3.3 French (Ono et al, 2020).

Comment R2.4 *The maximum error between phantom and CT image was 5.86 mm, which authors state is clinical acceptable. Please include comparison table with currently approved image co-registration modalities.*

Answer to R2.4 The CT and the phantom (present in EM tracking coordinates) were aligned using spherical fiducials. The registration error between the two systems was recorded to be less than 1mm. The vessel segmented from the CT was used as a ground truth to compare US reconstructed vessel thus evaluating the performance of our reconstruction pipeline. Results indicated that the vessel surface was off by 1.7 mm on average (confidence interval of 3.16 mm) with a few outliers where the error rose to 5.86 mm. This large error was observed in only one portion of the vessel, and was clearly seen as the vessel protruding out from one side.

While the average error is appropriate for an early-stage study, the maximum error is still quite high. We state that the errors reported in this study are acceptable based on a study by Linte et al. (2012) which conclude that for cardiovascular interventions, an error of up to 5mm is acceptable. According to clinicians in our team and authors, the accuracy constraints for IVC navigation are less strict than that.

That being said, there is room for improvement. The current error is largely due to the errors in the vessel segmentation step of the workflow. We have since developed a deep learning based segmentation technique with 90% accuracy. By replacing the traditional vessel segmentation technique used in this study with an advanced deep learning based segmentation algorithm, the entire vessel reconstruction can be made much more accurate. A reference to Linte et al. 2012 has been added to the Discussion section on page no. 14, line no. 265 as:

value (Linte et al., 2012). During navigation, it is important to identify

Comment R2.5 *There are minor grammatical issues.*

Answer to R2.5 Grammatical issues have been fixed.

Page no. 1, Abstract

Transcatheter **cardiovascular** interventions have the advantage of patient

Page no. 3, line no. 3.

procedural tools, have allowed surgical procedures to be performed

Page no. 5, line no. 51.

Procedures such as angioplasty, stent placement, **IVC filter placement**

Page no. 14, line no. 281.

origin of the image. The rigid and outer positioning of sensor **led** to some

Page no. 15, line no. 305.

require a robust deep learning-based segmentation **pipeline**, which is capable of

Page no. 4, line no. 35.

procedural navigation. CT is also based on ionizing radiation and carries the

Page no. 4, line no. 41.

fluoro methods and no-fluoro **procedural** workflows have also been proposed

Page no. 5, line no. 63.

most transcatheter interventions, there are two **interventional** phases -

Page no. 5, line no. 74.

imaging to navigate the tools, we propose the following **procedural** workflow

Page no. 13, line no. 260.

during **transcatheter** procedures. An EM-tracked ICE US probe was used

Page no. 1, Abstract

as **venography** or CT venography. These X-ray based techniques can have

Comment R2.6 *Manuscript could be shortened*

Answer to R2.6 The manuscript has been shortened by removing the equations for sensitivity and specificity as suggested.

Towards fluoro-free interventions: Using radial intracardiac ultrasound for vascular navigation

Hareem Nisar^{a,b,*}, Leah Groves^{a,b}, Leandro Cardarelli-Leite^c, Terry M. Peters^{a,b,d}, Elvis C.S. Chen^{a,b,d}

^a*Robarts Research Institute, Western University, London, ON, Canada*

^b*Department of Biomedical Engineering, Western University, London, ON, Canada*

^c*London Health Sciences Centre, London, ON, Canada*

^d*Department of Medical Biophysics, Western University, London, ON, Canada*

Abstract

Transcatheter cardiovascular interventions have the advantage of patient safety, reduced surgery time, and minimal trauma to the patient's body. Transcathether interventions, which are performed percutaneously are limited by the lack of direct line-of-sight with the procedural tools and the patient anatomy. Therefore, such interventional procedures rely heavily on image guidance for navigating towards and delivering therapy at the target site. Vascular navigation via the inferior vena cava (IVC), from the groin to the heart, is an imperative part of most transcatheter cardiovascular interventions including heart valve repair surgeries and ablation therapy. Traditionally, the IVC is navigated using fluoroscopic techniques such as venography or CT venography. These X-ray based techniques can have detrimental effects on the patient as well as the surgical team, causing increased radiation exposure, leading to risk of cancer, fetal defects, and eye

*Corresponding Author: Hareem Nisar, Robarts Research Institute, 1151 Richmond St. N. London, ON N6A 5B7; Email, hnисar3@uwo.ca; Phone, 519.931.5777

cataracts. The use of heavy lead apron has also been reported to cause back pain and spine issues thus leading to interventionalist's disc disease. We propose the use of a catheter-based ultrasound augmented with electromagnetic (EM) tracking technology to generate a vascular roadmap in real-time and perform navigation without harmful radiation. In this pilot study, we use spatially-tracked intracardiac echocardiography (ICE) to reconstruct a vessel from a phantom in a 3D virtual environment. We demonstrate how the proposed ultrasound-based navigation will appear in a virtual environment, by navigating a tracked guidewire within the vessels in the phantom without any radiation-based imaging. The geometric accuracy is assessed using a CT scan of the phantom, with a Dice coefficient of 0.79. The average distance between the surface of the two models comes out to be 1.7 ± 1.12 mm.

Keywords: Transcatheter interventions, Vascular navigation, Fluoro-free, Transfemoral guidance, Vascular Disease

1 Introduction

2 Advances in medical imaging, combined with miniaturized and flexible
3 procedural tools, have allowed surgical procedures to be performed percu-
4 taneously using transcatheter-based approaches. These minimally invasive
5 approaches have increased patient safety, decreased procedure time, and low-
6 ered complication rates (Jahangiri et al., 2019). Catheter-directed therapies
7 inherently prohibits the direct line-of-sight with the anatomy and the tools.
8 Interventionalists rely heavily on image-guidance to navigate and position
9 their tools to deliver therapy at the target region. Common imaging modal-
10 ities used for transcatheter-based interventions include X-ray fluoroscopy,
11 computed tomography (CT), magnetic resonance imaging (MRI), and in-
12 travascular (IVUS), intracardiac (ICE) or transesophageal (TEE) ultrasound
13 (US).

14 Fluoroscopy is commonly used for minimally invasive procedures as it pro-
15 vides real-time, high contrast vascular images, by means of X-ray imaging
16 with contrast enhancement. The radiation exposure produced by X-rays can
17 be harmful to the patient, clinical staff, and medical trainees, even when used
18 in conjunction with various shielding techniques (Theocharopoulos et al.,
19 2006; Christopoulos et al., 2016). The use of heavy shielding aprons may have
20 detrimental effects on the physical health of the interventional team causing
21 "interventionalist's disc disease" (Ross et al., 1997) which includes back and
22 neck pain (Dixon et al., 2017), cervical disc herniation, and other spinal and
23 musculoskeletal issues (Goldstein et al., 2004), as well as the possibility of
24 lead poisoning (Katsari et al., 2020). Interventional cardiologists and radiol-
25 ogists have reported developing eye cataracts (Jacob et al., 2013), increased

26 risk of cancer (Roguin et al., 2013), and increased risk of fetal congenital
27 defects (Limacher et al., 1998). The use of contrast agents to compensate
28 for the lack of soft-tissue visualization in X-rays can induce complications
29 for patients with renal impairments and allergic reactions (Davenport et al.,
30 2015).

31 Due to its high resolution and large field of view, pre-operative CT is
32 a standard of care for vascular mapping and assessment of intravascular
33 pathology (Murphy et al., 2018). However, CT imaging is typically used for
34 diagnostic and pre-surgical planning, and is limited in it's use for real-time
35 **procedural navigation**. CT is also based on ionizing radiation and carries the
36 same risks previously described for fluoroscopy. Furthermore, the surgery
37 cannot be performed with the patient within the CT bore. In transcatheter
38 procedures, there is an unmet need for safe, reliable, radiation-free and real-
39 time image-guidance during vascular navigation.

40 In efforts of minimizing the radiation exposure in Cath labs, near-zero
41 fluoro methods and no-fluoro **procedural workflows** have also been proposed
42 in the literature (Stec et al., 2014; Zhang et al., 2020) to guide the catheters
43 during an ablation procedure and perform transseptal puncture using ICE.
44 Alternative imaging modalities such as MR, and US are also considered.
45 Vascular navigation is fundamental to transcatheter cardiac interventions
46 such as transcatheter aortic valve implantation (TAVI), caval-valve implan-
47 tation, and mitral and tricuspid valve annuloplasty, repair and replacement
48 surgeries (Prendergast et al., 2019). Accurate representation of the vessel
49 geometry is not only important for navigation towards the target site, but
50 also for delivering the optimal therapy (Murphy et al., 2017; Shammas et al.,

51 2019). Procedures such as angioplasty, stent placement, IVC filter placement
52 all rely on vascular imaging to locate the pathological vessel region, select an
53 appropriately sized device, and deploy the balloon or stent correctly.

54 Catheter-based US technologies such as intravascular US (IVUS) and
55 intracardiac echo (ICE) are already indispensable components of Cardiac
56 Catheterization labs (Cath Lab), assisting in the assessment of the disease
57 and device placement. The recent introduction of optical US (OpUS) tech-
58 nology also shows the great potential for the use of catheter-based US for
59 cardiovascular interventions (Little et al., 2020). US offers a radiation-free
60 alternative for real-time image guidance. When combined with EM tracking
61 technology, it offers the potential for a large-scale 3D US volume recon-
62 struction, visualization of anatomy, as well as real-time tool tracking. For
63 most transcatheter interventions, there are two interventional phases - nav-
64 igation of tools towards the target site and positioning of tools to deliver
65 the treatment. In the case of cardiac interventions, vascular navigation is
66 an imperative prerequisite. Either transfemoral, transradial or transjugular
67 access is required to guide the catheters towards the heart. Inferior vena
68 cava (IVC) navigation, from the groin to the chest, is one of the most com-
69 mon techniques in cardiology and is traditionally guided by fluoroscopy. In
70 this paper, the targeted clinical application is the IVC navigation performed
71 during transcatheter cardiovascular interventions.

72 We propose the use of tracked US as an alternative to CT-based vascular
73 mapping and fluoro-guided tool navigation. Instead of using radiation-based
74 imaging to navigate the tools, we propose the following procedural workflow:
75 Prior to the intervention, a tracked, catheter-based US probe (such as ICE,

76 IVUS, or OpUS) scans the desired vasculature and a virtual 3D roadmap is
77 reconstructed. This vascular path can then be easily traversed by a tracked
78 tool or guidewire. This workflow eliminates radiation exposure and the use
79 of heavy lead equipment. Such a system can also be used to make measure-
80 ments of the vessel anatomy and intraluminal buildup. Ultrasound catheters
81 including ICE and IVUS, as well as EM tracking technology are already an
82 indispensable part of a Cath Lab and are used in electrophysiology proce-
83 dures. The proposed ultrasound-based workflow has several advantages over
84 the conventional fluoroscopic techniques. Apart from the lack of radiation,
85 and heavy lead shielding equipment, an US-based navigation system offers
86 full 3D visualization of anatomy, and provides more information to the clin-
87 ician. Furthermore, the use of EM tracking technology allows for tracked
88 tools and catheters which can result in an engaged and informative experi-
89 ence for the clinicians. These features greatly reduce the cognitive load faced
90 by the interventionalists and will potentially result in enhanced procedural
91 outcome as well.

92 In this study, we utilized a Foresight ICE system – an intracardiac ul-
93 trasound probe which involves a single-element transducer, spinning on its
94 axis and tilted at a user-specified angle. As a result, the ultrasound image
95 produced is a 2D conical surface image lying in 3D space. One of the biggest
96 advantages of using this probe for navigation is the ‘Forward-viewing’ feature
97 which allows the clinicians to watch where they are going as they traverse
98 the vessels, thus improving their experience and adding a layer of procedural
99 safety. The use of ICE probe is not limited to navigation. For transcatheter
100 cardiac interventions, the ultrasound can further facilitate the delivery of

101 therapy or treatment. This study is geared towards the navigation of inferior
102 vena cava (IVC), it also has the potential to be applied to the navigation
103 of other vessels as well. IVC has many tributaries, but they need not to
104 be navigated for cardiac procedures. The geometry of IVC is also compar-
105 atively simpler than its tributaries like hepatic veins. Since the IVC passes
106 through the entire length of the abdomen, it's surrounding tissues and organs
107 vary along the length. Thus, the appearance of the IVC in the ultrasound
108 varies as well. All these physical and echogenic attributes of IVC are diffi-
109 cult to capture in one phantom. Therefore, for this first, phantom study we
110 are demonstrating the concept on an ultrasound-realistic phantom represent-
111 ing the infrarenal portion of the IVC. The goal is to reconstruct a vascular
112 roadmap without any radiations, safely navigate the guidewire through the
113 vessel, and visualize the guiding catheters as they ascend towards the heart.

114 This paper presents a pilot phantom study as a proof of concept to
115 demonstrate the idea and feasibility of an US-based vascular navigation sys-
116 tem for transcatheter interventions. A vascular phantom was scanned and
117 reconstructed using a forward-looking radial ICE probe and EM tracking
118 technology. The method details, open-source implementation, and phan-
119 tom images are available online for reproducibility (<https://github.com/hareem-nisar/VascularNavigation>). The US-generated vessel model is
120 validated against a CT-scan of the vessel phantom. For a visual validation
121 and concept demonstration of real-time guidance, we also demonstrate nav-
122 igation of a tracked guide-wire in a vascular phantom using the proposed
123 US-based approach.

125 **Materials and Methods**

126 *Data Acquisition*

127 A polyvinyl alcohol cryogel (PVA-C) vascular phantom was manufactured
128 to imitate the infra-renal portion of the IVC (Nisar et al., 2020). The phan-
129 tom generated realistic US imaging when scanned by an intravascular (IVUS)
130 or intracardiac (ICE) US, thus displaying a vessel-mimicking layer, blood-
131 mimicking fluid in the lumen, and a surrounding tissue-mimicking layer. In
132 this study, a 10 Fr, forward-looking, Foresight™(Conavi Medical Inc., North
133 York, ON, Canada) ICE catheter was used to image the phantom. This
134 probe generates 3D conical surface images, where the angle of the cone is
135 user adjustable. The conical images are projected on a conventional monitor
136 screen as viewed from the apex of the cone and displayed as a circular im-
137 age. A digital frame-grabber (DVI2USB 3.0, Epiphan Video, Ottawa, ON,
138 Canada) was used to capture the projected ICE images, and the cone-angle
139 information from the console. For US tracking, the ICE probe was rigidly in-
140 strumented with a 6DoF pose sensor (Aurora, NDI, Waterloo, ON, Canada)
141 and spatially calibrated using a point-to-line Procrustean approach (Chen
142 et al., 2016; Nisar et al., 2019).

143 The vessel phantom was placed in a large water-bath at room-temperature
144 (Fig. 1). The main vessel of the phantom was scanned using the tracked
145 ICE probe at an imaging depth of 80 mm, imaging angle of 67 ° and 12 MHz
146 frequency. Due to some hardware constraints in our set-up, we were only
147 able to scan the central vessel of the phantom and not the branches (details
148 in Discussion section). US images were acquired in real-time using screen-
149 capture. The imaging and tracking data were then processed to reconstruct

150 the surface representation of the vessel from the phantom. The data acqui-
151 sition, vascular roadmap generation, and the user interface for navigation
152 were all implemented as an open-source software using 3D Slicer (Fedorov
153 et al., 2012). The steps involved in the automatic generation of the 3D
154 vascular roadmap include pre-processing to remove image artifacts, lumen
155 segmentation from 2D images and reconstruction of the vessel based on the
156 segmentations and tracking information.

157 *Pre-processing*

158 The acquired screen-captures were cropped to remove any information
159 outside of the US image. The bright reflections in the middle of the cropped
160 US image represent an artifact inherent to the ICE probe (Fig. 2a). This
161 artifact was minimized by using optimal display settings (third level 'wand'
162 function) on the console, and later masking the central bright pixels in the
163 image in our software. The time-gain compensation settings on the console
164 were used to suppress the reflections from the phantom boundary and the
165 container walls. A noise removing filter called the curve flow filter was applied
166 to images to eliminate the interference from by the EM tracker (Fig. 2a) while
167 preserving the contours of the vessel boundary. This was a necessary step
168 prior to performing image processing for lumen segmentation.

169 *Lumen Segmentation*

170 Distinct from imaging using hand-held percutaneous US transducer, the
171 shape of the vessel wall can vary significantly for catheter-based US. Since the
172 US catheters travel through the vasculature adhering close to the vessel wall,
173 the wall does not always appear as a closed circle in the case of radial IVUS

and ICE imaging. The first few millimeters of ICE imaging are corrupted by a ring artifact inherent to the radial ICE probe (Fig. 2a). As such, when the ICE catheter is clinging to the vessel wall, the reflection is interrupted close to the center of the image (Fig. 2a) and the vessel boundary appears C-shaped. Therefore, in this study, an edge-based approach was used to segment the vessel lumen from the ICE images, minimizing the error/leakages caused by a discontinuous vessel boundary. A statistics-based active contour algorithm was applied (Gao et al., 2010). This algorithm grows the boundaries of an initial seed based on the characteristics of the underlying image intensities, and can be manipulated by the parameters ‘intensity homogeneity’ (set to 0.8) and ‘boundary smoothness’ (set to 1) to maintain the roundness of the contour and minimize leakages based on intensity.

The performance of the segmentation algorithm is highly dependent on the size and placement of the initial seed. Therefore, for the algorithm to be effective, it is necessary to have an initial seed, closely fitted to and completely encapsulated and centered within the vessel lumen (Gao et al., 2010). The Hough transform was used to approximate the initial seed by fitting a circle to the lumen (Fig. 2b) (Parameters values: Hough Gradient, $dp = 1$, $\text{min_dist} = 100$, $\text{param1} = 95$, $\text{param2} = 20$). Gaussian blur was applied prior to the Hough transform to avoid over-detection of circles. To ensure that the seed does not overlap with the vessel boundary, the fitted circle was iteratively decreased in radius until there were no bright reflections in the underlying image. A hundred and eighty image frames were processed and 2D lumen segmentations were acquired for each image.

198 *Vessel Reconstruction*

199 The Foresight™ICE probe generates forward-looking conical surface im-
 200 ages. The images acquired by this device, and subsequently the lumen seg-
 201 mentation, were a version of the true US data projected onto a 2D disk. 2D
 202 lumen segmentations were subjected to 3D conversion to reconstruct true,
 203 conical segmentations (Fig. 2c) using the radius and imaging angle informa-
 204 tion, available through the console. This reconstruction is governed by the
 205 equation:

$$\begin{bmatrix} x_{3D} \\ y_{3D} \\ z_{3D} \end{bmatrix} = \begin{bmatrix} 1 & 0 & -o_x \\ 0 & 1 & -o_y \\ 0 & 0 & \|(x_{2D}, y_{2D})\| \cdot \tan(90 - \phi) \end{bmatrix} \begin{bmatrix} x_{2D} \\ y_{2D} \\ 1 \end{bmatrix} \quad (1)$$

206 where (o_x, o_y) represents the center of the planar image or the apex of the
 207 conical image, and ϕ represents the imaging angle of the cone-shaped im-
 208 age. Each segmentation was positioned and scaled to its correct shape and
 209 location in 3D space by applying US probe calibration and tracking infor-
 210 mation, producing a skeleton of the vessel (Fig. 3a). The vessel skeleton
 211 was then processed to form a closed 3D surface representation using binary
 212 morphological closing, with an annulus kernel of size [60, 60] to fill the gaps
 213 between consecutive segments. For final smoothing of the reconstructed ves-
 214 sel, a Gaussian blur with a standard deviation of 3 was applied. The result
 215 represents the 3D model of the vessel scanned from our phantom (Fig. 3b),
 216 spatially present in the EM tracker's coordinate system.

217 *Validation*

218 As described previously, vascular navigation is currently achieved using
219 fluoroscopy or CT mapping. The vessel phantom was imaged using US, and
220 the vessel was reconstructed and compared with X-ray and CT. Geomet-
221 ric accuracy of the US reconstructed vessel model was validated against the
222 vessel segmented from the CT scan of the same phantom. The absolute
223 surface-to-surface distance between the two models were computed after a
224 rigid registration (Besl and McKay, 1992). For vascular navigation, one of
225 the clinically relevant goals is to know the overall alignment of the vessels
226 in space. To evaluate the spatial alignment, we used DICE metrics which
227 compares the spatial overlap between the reconstructed and CT vessel af-
228 ter CT-US registration was performed. False positive spatial region in the
229 reconstructed US vessel is also an important metric and must be minimal
230 to avoid the misrepresentation of the vessel. For many vascular procedures,
231 the clinical objective is to avoid puncturing the vessels. In such cases, the
232 boundary accuracy becomes important as well as the false positive regions.
233 To evaluate the contours of the reconstructed vessel, we calculated the Haus-
234 dorff distance (HD) metrics (Taha and Hanbury, 2015). Volumetric analysis
235 was not performed as volume-based metrics are invariant of segmentation
236 shape and boundary and thus can be misleading. As a visual validation, we
237 demonstrate what US-based navigation may look like. A tracked, straight-
238 tip guidewire(Piazza et al., 2020), augmented with a 5DOF EM sensor, was
239 maneuvered to navigate the vessels in the phantom.

240 **Results**

241 The absolute distance between the US reconstructed vessel and the reg-
242 istered CT segmented vessel was computed and presented as a heatmap on
243 the vessel surface in Fig. 3c. The average distance between the surface of
244 the two models comes out to be 1.7 ± 1.12 mm. A maximum error of 5.86 mm
245 between the two surface models was observed. The spatial overlap between
246 the registered US and CT models was evaluated using the Dice coefficient,
247 sensitivity and specificity measures where

$$Dice = \frac{\text{True positive overlap between CT and US vessels}}{(\text{num voxels CTvessel}) * (\text{num voxels USvessel})} \quad (2)$$

248 The spatial distance between the two model boundaries was evaluated
249 using the Hausdorff distance (HD). The geometric accuracy results are re-
250 ported in Table 1. Comparison showed that the US model had 12.93 % false
251 negative and 6.60 % false positive spatial overlap.

252 The x-ray imaging of our phantom, along with a guidewire, is represented
253 in Fig. 4a. In comparison, we can also achieve tool guidance using an US-
254 guided vascular navigation system. Fig. 4b shows how the US reconstructed
255 vessel looks like in 3D space. Virtual representation of a tracked guidewire
256 can be seen in context, as it navigates the phantom vessel.

257 **Discussion**

258 In this study, we present an vascular reconstruction-based navigation
259 system, which provides a safe and radiation-free method for guiding tools
260 during **transcatheter procedures**. An EM-tracked ICE US probe was used

261 to reconstruct the vascular path in a phantom, such that it can be visu-
262 alized in a common coordinate system with a tracked guidewire for vessel
263 navigation. The results indicate that the average error in terms of HD is
264 1.7 mm, with a 3.16 mm confidence interval, which is a clinically acceptable
265 value (Linte et al., 2012). During navigation, it is important to identify
266 the vessel boundary and the regions outside the vessel lumen so as to not
267 puncture or damage the vessel wall. Our results indicate that only 6.60 %
268 region lies outside the ground truth provided by the CT scan of the phantom.
269 This over-segmentation is due to the leakages through the discontinuous wall
270 boundary in some of the images when the ultrasound probe is clinging to the
271 vessel wall. The accuracy of the navigation system can further be improved
272 by improving the segmentation and tracking accuracy as discussed below.

273 The resulting error is a combination of many different errors in the sys-
274 tem, such as EM tracking inaccuracies, propagation of calibration errors, US
275 probe hardware constraints, registration errors, and relative motion of the
276 phantom if any. One of the major limitations of our study is defined by the
277 sensorizing the US probe and its calibration accuracy. This inaccuracy can
278 be minimized by applying a manual offset correction for the imaging angle.
279 The ICE probe used in this study has a small diameter of 3.3 mm which re-
280 quired rigidly fixing the sensor on the outer sheath of the probe, farther away
281 from the origin of the image. The rigid and outer positioning of sensor led
282 to some hardware constraints resulting in our inability to turn and guide the
283 probe into the branches of the vessel. This limitation is strictly a character-
284 istic of our experimental setup in this preliminary study using a Foresight™
285 ICE probe. The proposed idea can be extended to other radial ultrasound

286 catheters as well. Ideally the tracking sensor should be integrated within
287 the US catheter and pre-calibrated by the manufacturers to eliminate any
288 limitation of maneuvering the US. For a clinical system, the EM sensor must
289 be integrated inside the US catheter to achieve accuracy in tracking, free-
290 dom in motion and patient safety from an active element. In the future, we
291 plan to collaborate with the ICE probe manufacturers to acquire ICE probes
292 embedded with EM sensors and designing a prototype of the US guidance
293 system presented as a concept study in this paper.

294 The proposed US-based vascular navigation system can be implemented
295 using many catheter-based US technology, such as radial IVUS probes that
296 are regularly used during cardiac and endovascular interventions. Other than
297 tracking, the accuracy of a clinical vessel reconstruction algorithm will also
298 largely depend on the accuracy of lumen segmentation from in-vivo imaging.
299 The appearance of a vessel in an intravascular or intracardiac US image varies
300 significantly depending on the size and composition of the vessel, as well as
301 the surrounding tissue and organs. The phantom images presented in this
302 study replicate the US imaging of the infrarenal portion of IVC only. Even
303 the echogenicity of the IVC changes as it passes through the abdomen. Thus
304 a clinical system, implementing the proposed idea of US navigation, will re-
305 quire a robust deep learning-based segmentation pipeline, which is capable of
306 accurately identifying and segmenting all vascular structures as well as ves-
307 sel branches and tributaries. Existing network architectures, such as U-Net,
308 might be a suitable option for medical image segmentation. Since this is a
309 pilot, proof of concept study for navigation with relatively restricted imaging
310 data, we did not include any learning based approaches for segmentation and

311 relied on conventional image processing techniques.

312 In future work we aim to improve this vascular reconstruction pipeline
313 by replacing the image-processing based vessel segmentation algorithm with
314 a deep learning-based segmentation technique trained on animal images ac-
315 quired using the forward-looking, Foresight™ICE probe. The use of machine-
316 learning for vascular segmentation and reconstruction has been previously
317 performed using both surface US scans (Groves et al., 2020; Yang et al.,
318 2013) and intravascular US (Yang et al., 2018). The integration of a machine-
319 learning based segmentation will allow for accurate patient specific recon-
320 structions to be obtained that account for differences in patients pathology.
321 The segmentation algorithm can be trivially replaced within our vascular re-
322 construction pipeline such that the different vessels required for navigation
323 can be reconstructed using a robust segmentation algorithm capable of de-
324 lineating various vascular morphologies and side vessel branches, allowing for
325 safe navigation from the insertion site to the central venous system.

326 The phantom based workflow presented in this paper is time consuming
327 due to the computationally expensive vessel segmentation technique used.
328 For clinical purposes, the vessel segmentation step should be fast and robust.
329 However, this is a first proof of concept study and the vessel segmentation
330 step is only suitable for the phantom images. Therefore, to replace the cur-
331 rent vessel segmentation step, we have developed a real-time segmentation
332 technique for isolating vessel lumina from ultrasound imaging of inferior vena
333 cava in animals.¹. We are also currently working towards optimizing the

¹The preprint has been made available at research gate (DOI: 10.13140/RG.2.2.31644.82567)

334 presented pipeline to perform the vessel reconstruction in order of seconds.
335 Combining the optimized reconstruction algorithm with the real-time vessel
336 segmentation method will enable a time-apt image guidance system ready
337 for pre-clinical studies.

338 The accuracy of the vessel reconstruction algorithm presented in this
339 paper largely depends on the accuracy of the vessel segmentation and the
340 tracking technology used. The electromagnetic tracking has submillimeter
341 accuracy, however the vessel segmentation does not. As mentioned earlier,
342 we have developed a real-time vessel segmentation method using deep learn-
343 ing. This new segmentation method relies on a trained U-net model to accu-
344 rately segment the complex-shaped vessel lumina from the ICE imaging of the
345 vena cava from a swine. This deep learning based method is robust against
346 boundary artifacts such as intraluminal buildups and stents. However, the
347 algorithm produce inaccurate segmentation when a lead is present inside the
348 vessel. Any artifacts outside the vessel and present in the surrounding tissue
349 do not have a significant impact on the accuracy of our vessel segmentation
350 and reconstruction. To cater for the any artefacts, the new segmentation
351 technique can be trivially modified without disturbing the entire reconstruc-
352 tion pipeline presented in this paper. Deep learning based systems benefit
353 from a variety of imaging datasets in making the segmentation algorithm
354 more robust. By retraining the U-net model on different examples of vascu-
355 lar imaging with artifacts, the segmentation and thus the reconstruction can
356 be made robust and accurate.

357 Another limitation is the size of the US catheter. The US probe used in
358 this study is a 10 Fr device which is large and less suitable for the arterial

359 system, although it is usually not problematic for venous interventions. This
360 is a limitation of the current technology (Foresight™ ICE probe by Conavi
361 Medical Inc.) and ideally this device will be miniaturized by the manufactur-
362 ers in the near future. The workflow presented in this paper can potentially
363 be adapted for intravascular ultrasound (IVUS) imaging where the catheter is
364 much smaller. For example, the Novasight Hybrid (by Conavi Medical Inc.)
365 is a combined IVUS-OCT imaging catheter with a size of 3.3 French (Ono
366 et al., 2020).

367 **Conclusions**

368 Transcatheter interventions provide a low-impact means of delivering
369 therapy using miniaturized equipment and medical imaging technologies.
370 Vascular navigation is a ubiquitous process as it is a prerequisite to reach the
371 target organ or target site in another vessel. The current standard of care
372 employs fluoroscopic techniques or the use of CT vascular mapping, both
373 of which come at a cost of radiation exposure and wearing heavy, shielding
374 aprons. Through this study, we aim to initiate a discussion on the merits
375 of moving towards the use of ultrasound-based instead of radiation-based
376 techniques for transcatheter and endovascular interventions. We present a
377 proof of concept study to use catheter-based US technology, equipped with
378 tracking sensors, to create a vascular roadmap. Results indicate that the
379 geometric accuracy is comparable to that observed in CT mapping. The
380 concept demonstration (Fig. 4) shows side by side that an US-guided system
381 can provide the same level of information and in three dimensions without
382 the hazards of radiation and lead shielding.

383 Acknowledgements

384 The authors would like to thank Dr. Dan Bainbridge (London Health
385 Sciences Centre) and John Moore (Archetype Biomedical Inc.) for their
386 valuable discussion and insight into the project. We acknowledge our sources
387 of funding - Canadian Institutes of Health Research (CIHR) and Candaian
388 Foundation for Innovation (CFI). The grants are held by Dr. Terry Peters.
389 The authors would also like to thank Conavi Medical Inc. for providing the
390 ultrasound imaging dataset.

391 **References**

- 392 Besl P, McKay ND. A method for registration of 3-d shapes. IEEE Transactions on Pattern Analysis and Machine Intelligence, 1992;14:239–256.
- 393
- 394 Chen ECS, Peters TM, Ma B. Guided ultrasound calibration: where, how, and how many calibration fiducials. International Journal of Computer Assisted Radiology and Surgery, 2016;11:889–898.
- 395
- 396
- 397 Christopoulos G, Makke L, Christakopoulos G, Kotsia A, Rangan BV, Roesle M, Haagen D, Kumbhani DJ, Chambers CE, Kapadia S, Mahmud E, Banerjee S, Brilakis ES. Optimizing Radiation Safety in the Cardiac Catheterization Laboratory. Catheterization and Cardiovascular Interventions, 2016;87:291–301.
- 398
- 399
- 400
- 401
- 402 Davenport MS, Cohan RH, Ellis JH. Contrast Media Controversies in 2015: Imaging Patients With Renal Impairment or Risk of Contrast Reaction. American Journal of Roentgenology, 2015;204:1174–1181.
- 403
- 404
- 405 Dixon RG, Khiatani V, Statler JD, Walser EM, Midia M, Miller DL, Bartal G, Collins JD, Gross KA, Stecker MS, Nikolic B. Society of Interventional Radiology: Occupational Back and Neck Pain and the Interventional Radiologist. Journal of Vascular and Interventional Radiology, 2017;28:195–199.
- 406
- 407
- 408
- 409 Fedorov A, Beichel R, Kalpathy-Cramer J, Finet J, Fillion-Robin JC, Pu-jol S, Bauer C, Jennings D, Fennessy F, Sonka M, Buatti J, Aylward S, Miller JV, Pieper S, Kikinis R. 3D Slicer as an image computing platform for the Quantitative Imaging Network. Magnetic resonance imaging, 2012;30:1323–41.
- 410
- 411
- 412
- 413

- ⁴¹⁴ Gao Y, Tannenbaum A, Kikinis R. Simultaneous multi-object segmentation using local robust statistics and contour interaction. In: International
⁴¹⁵ MICCAI Workshop on Medical Computer Vision. Springer, 2010. pp. 195–
⁴¹⁶ 203.
- ⁴¹⁷
- ⁴¹⁸ Goldstein JA, Balter S, Cowley M, Hodgson J, Klein LW. Occupational hazards of interventional cardiologists: Prevalence of orthopedic health problems in contemporary practice. *Catheterization and Cardiovascular Interventions*, 2004;63:407–411.
- ⁴¹⁹
- ⁴²⁰
- ⁴²¹
- ⁴²² Groves LA, VanBerlo B, Veinberg N, Alboog A, Peters TM, Chen EC. Automatic segmentation of the carotid artery and internal jugular vein from
⁴²³ 2d ultrasound images for 3d vascular reconstruction. *International journal of computer assisted radiology and surgery*, 2020.
- ⁴²⁴
- ⁴²⁵
- ⁴²⁶ Jacob S, Boveda S, Bar O, Brézin A, Maccia C, Laurier D, Bernier MO. Interventional cardiologists and risk of radiation-induced cataract: Results
⁴²⁷ of a French multicenter observational study. *International Journal of Cardiology*, 2013;167:1843–1847.
- ⁴²⁸
- ⁴²⁹
- ⁴³⁰ Jahangiri M, Hussain A, Akowuah E. Minimally invasive surgical aortic valve
⁴³¹ replacement. *Heart*, 2019;105:s10–s15.
- ⁴³²
- ⁴³³
- ⁴³⁴
- ⁴³⁵ Katsari K, Paraskevopoulou C, Barati M, Kostopoulou E, Griskevicius R, Blazquez N, Tekin HO, Illing RO. Lead exposure in clinical imaging—the elephant in the room. *European Journal of Radiology*, 2020;131:109210.
- ⁴³⁶
- ⁴³⁷ Limacher MC, Douglas PS, Germano G, Laskey WK, Lindsay BD, Mcketty MH, Moore ME, Park JK, Prigent FM, Walsh MN, Forrester JS, Faxon

- 437 DP, Fisher JD, Gibbons RJ, Halperin JL, Hutter AM, Kaul S, Skorton DJ,
438 Weintraub WS, Winters WL, Wolk MJ. Radiation Safety in the Practice
439 of Cardiology. Tech. rep., 1998.
- 440 Linet CA, Lang P, Rettmann ME, Cho DS, Holmes DR, Robb RA, Peters
441 TM. Accuracy Considerations in Image-guided Cardiac Interventions: Ex-
442 perience and Lessons Learned. International journal of computer assisted
443 radiology and surgery, 2012;7:13.
- 444 Little CD, Colchester RJ, Noimark S, Manmathan G, Finlay MC, Desjardins
445 AE, Rakhit RD. Optically generated ultrasound for intracoronary imaging.
446 Frontiers in Cardiovascular Medicine, 2020;7.
- 447 Murphy DJ, Aghayev A, Steigner ML. Vascular CT and MRI: a practical
448 guide to imaging protocols. Insights into Imaging, 2018;9:215–236.
- 449 Murphy EA, Ross RA, Jones RG, Gandy SJ, Aristokleous N, Salsano M,
450 Weir-McCall JR, Matthew S, Houston JG. Imaging in Vascular Access.
451 Cardiovascular Engineering and Technology, 2017;8:255–272.
- 452 Nisar H, Moore J, Alves-Kotzev N, Hwang GYS, Peters TM, Chen ECS.
453 Ultrasound calibration for unique 2.5D conical images. In: Fei B, Linet
454 CA (Eds.), Medical Imaging 2019: Image-Guided Procedures, Robotic
455 Interventions, and Modeling. SPIE, 2019. p. 78.
- 456 Nisar H, Moore J, Piazza R, Maneas E, Chen ECS, Peters TM. A sim-
457 ple, realistic walled phantom for intravascular and intracardiac applica-
458 tions. International Journal of Computer Assisted Radiology and Surgery,
459 2020;15:1513–1523.

- ⁴⁶⁰ Ono M, Kawashima H, Hara H, Gao C, Wang R, Kogame N, Takahashi K,
⁴⁶¹ Chichareon P, Modolo R, Tomaniak M, Wykrzykowska JJ, Piek JJ, Mori
⁴⁶² I, Courtney BK, Wijns W, Sharif F, Bourantas C, Onuma Y, Serruys
⁴⁶³ PW. Advances in IVUS/OCT and Future Clinical Perspective of Novel
⁴⁶⁴ Hybrid Catheter System in Coronary Imaging. *Frontiers in Cardiovascular
465 Medicine*, 2020;7:119.
- ⁴⁶⁶ Piazza R, Nisar H, Moore J, Condino S, Ferrari M, Ferrari V, Peters T,
⁴⁶⁷ Chen E. Towards electromagnetic tracking of J-tip guidewire: precision
⁴⁶⁸ assessment of sensors during bending tests. In: Fei B, Linte CA (Eds.),
⁴⁶⁹ Medical Imaging 2020: Image-Guided Procedures, Robotic Interventions,
⁴⁷⁰ and Modeling. SPIE, 2020. p. 5.
- ⁴⁷¹ Prendergast BD, Baumgartner H, Delgado V, Gérard O, Haude M, Him-
⁴⁷² melmann A, Iung B, Leafstedt M, Lennartz J, Maisano F, Marinelli EA,
⁴⁷³ Modine T, Mueller M, Redwood SR, Rörick O, Sahyoun C, Saillant E,
⁴⁷⁴ Søndergaard L, Thoenes M, Thomitzek K, Tschernich M, Vahanian A,
⁴⁷⁵ Wendler O, Zemke EJ, Bax JJ. Transcatheter heart valve interventions:
⁴⁷⁶ where are we? Where are we going? *European Heart Journal*, 2019;40:422–
⁴⁷⁷ 440.
- ⁴⁷⁸ Roguin A, Goldstein J, Bar O, Goldstein JA. Brain and Neck Tumors Among
⁴⁷⁹ Physicians Performing Interventional Procedures. *The American Journal
480* of Cardiology
- ⁴⁸¹ Ross AM, Segal J, Borenstein D, Jenkins E, Cho S. Prevalence of Spinal
⁴⁸² Disc Disease Among Interventional Cardiologists. *The American Journal
483* of Cardiology

- 484 Shammas N, Radaideh Q, Shammas WJ, Daher GE, Rachwan RJ, Radaideh
485 Y. The role of precise imaging with intravascular ultrasound in coro-
486 nary and peripheral interventions. Vascular Health and Risk Management,
487 2019;Volume 15:283–290.
- 488 Stec S, Śledz J, Mazij M, Ras M, Ludwik B, Chrabaszcz M, Śledz A, Ba-
489 nasik M, Bzymek M, Mlynarczyk K, Deutsch K, Labus M, Śpikowski J,
490 Szydłowski L. Feasibility of Implementation of a “Simplified, No-X-Ray,
491 No-Lead Apron, Two-Catheter Approach” for Ablation of Supraventricu-
492 lar Arrhythmias in Children and Adults. Journal of Cardiovascular Elec-
493 trophysiology, 2014;25:866–874.
- 494 Taha AA, Hanbury A. Metrics for evaluating 3D medical image segmentation:
495 analysis, selection, and tool. BMC Medical Imaging, 2015;15:29.
- 496 Theocharopoulos N, Damilakis J, Perisinakis K, Manios E, Vardas P, Gourt-
497 soyiannis N. Occupational exposure in the electrophysiology laboratory:
498 quantifying and minimizing radiation burden. The British Journal of Ra-
499 diology, 2006;79:644–651.
- 500 Yang J, Tong L, Faraji M, Basu A. Ivus-net: an intravascular ultrasound
501 segmentation network. In: International Conference on Smart Multimedia.
502 Springer, 2018. pp. 367–377.
- 503 Yang X, Jin J, Xu M, Wu H, He W, Yuchi M, Ding M. Ultrasound common
504 carotid artery segmentation based on active shape model. Computational
505 and mathematical methods in medicine, 2013;345968.

506 Zhang G, Cheng L, Liang Z, Zhang J, Dong R, Hang F, Wang X,
507 Wang Z, Zhao L, Wang Z, Wu Y. Zero-fluoroscopy transseptal puncture
508 guided by right atrial electroanatomical mapping combined with intrac-
509 ardiac echocardiography: A single-center experience. Clinical Cardiology,
510 2020;43:1009–1016.

511 **Figure Captions**

512 **Figure 1:** Data acquisition setup - Ultrasound probe scans the vessel phan-
513 tom present within the tracking space.

514 **Figure 2:** (a) Image data acquired using a framegrabber as a 2D projec-
515 tion of the conical ultrasound. (b) Lumen segmentation (boundary)
516 achieved using the initial seed (solid). (c) Conical reconstruction of the
517 ultrasound image and the lumen segmentation.

518 **Figure 3:** Image a) depicts the skeleton of the vessel comprised of spatially
519 calibrated segmentations, Image b) depicts the ultrasound (US) re-
520 construction registered to the segmented CT scan of the phantom, and
521 Image c) provides a visualization of the surface-to-surface distance anal-
522 ysis between the US and CT models.

523 **Figure 4:** An example use case for navigating a tracked guidewire within the
524 ultrasound reconstructed vessel (b) as compared to the fluoroscopic
525 equivalent (a)

526 **Tables**

527 **Table 1:** Summary of the metrics use to quantify The spatial overlap and
528 boundary accuracy of the ultrasound reconstructed vessel compared to
529 the vessel segmented from the CT scan of the phantom.

Spatial Overlap	Value	Hausdorff Distance (mm)	Value
DICE Coefficient	0.79	Maximum	5.86
Sensitivity	0.70	Average	1.63
Specificity	0.88	95 %	3.16

Towards fluoro-free interventions: Using radial intracardiac ultrasound for vascular navigation

Hareem Nisar^{a,b,*}, Leah Groves^{a,b}, Leandro Cardarelli-Leite^c, Terry M. Peters^{a,b,d}, Elvis C.S. Chen^{a,b,d}

^a*Robarts Research Institute, Western University, London, ON, Canada*

^b*Department of Biomedical Engineering, Western University, London, ON, Canada*

^c*London Health Sciences Centre, London, ON, Canada*

^d*Department of Medical Biophysics, Western University, London, ON, Canada*

Abstract

Transcatheter cardiovascular interventions have the advantage of patient safety, reduced surgery time, and minimal trauma to the patient's body. Transcathether interventions, which are performed percutaneously are limited by the lack of direct line-of-sight with the procedural tools and the patient anatomy. Therefore, such interventional procedures rely heavily on image guidance for navigating towards and delivering therapy at the target site. Vascular navigation via the inferior vena cava (IVC), from the groin to the heart, is an imperative part of most transcatheter cardiovascular interventions including heart valve repair surgeries and ablation therapy. Traditionally, the IVC is navigated using fluoroscopic techniques such as venography or CT venography. These X-ray based techniques can have detrimental effects on the patient as well as the surgical team, causing increased radiation exposure, leading to risk of cancer, fetal defects, and eye

*Corresponding Author: Hareem Nisar, Robarts Research Institute, 1151 Richmond St. N. London, ON N6A 5B7; Email, hnисar3@uwo.ca; Phone, 519.931.5777

cataracts. The use of heavy lead apron has also been reported to cause back pain and spine issues thus leading to interventionalist's disc disease. We propose the use of a catheter-based ultrasound augmented with electromagnetic (EM) tracking technology to generate a vascular roadmap in real-time and perform navigation without harmful radiation. In this pilot study, we use spatially-tracked intracardiac echocardiography (ICE) to reconstruct a vessel from a phantom in a 3D virtual environment. We demonstrate how the proposed ultrasound-based navigation will appear in a virtual environment, by navigating a tracked guidewire within the vessels in the phantom without any radiation-based imaging. The geometric accuracy is assessed using a CT scan of the phantom, with a Dice coefficient of 0.79. The average distance between the surface of the two models comes out to be 1.7 ± 1.12 mm.

Key words: Transcatheter interventions, Vascular navigation, Fluoro-free, Transfemoral guidance, Vascular Disease

1 Introduction

2 Advances in medical imaging, combined with miniaturized and flexible
3 procedural tools, have allowed surgical procedures to be performed percu-
4 taneously using transcatheter-based approaches. These minimally invasive
5 approaches have increased patient safety, decreased procedure time, and low-
6 ered complication rates (?). Catheter-directed therapies inherently prohibits
7 the direct line-of-sight with the anatomy and the tools. Interventionalists rely
8 heavily on image-guidance to navigate and position their tools to deliver ther-
9 apy at the target region. Common imaging modalities used for transcatheter-
10 based interventions include X-ray fluoroscopy, computed tomography (CT),
11 magnetic resonance imaging (MRI), and intravascular (IVUS), intracardiac
12 (ICE) or transesophageal (TEE) ultrasound (US).

13 Fluoroscopy is commonly used for minimally invasive procedures as it
14 provides real-time, high contrast vascular images, by means of X-ray imag-
15 ing with contrast enhancement. The radiation exposure produced by X-rays
16 can be harmful to the patient, clinical staff, and medical trainees, even when
17 used in conjunction with various shielding techniques (??). The use of heavy
18 shielding aprons may have detrimental effects on the physical health of the
19 interventional team causing "interventionalist's disc disease" (?) which in-
20 cludes back and neck pain (?), cervical disc herniation, and other spinal and
21 musculoskeletal issues (?), as well as the possibility of lead poisoning (?).
22 Interventional cardiologists and radiologists have reported developing eye
23 cataracts (?), increased risk of cancer (?), and increased risk of fetal con-
24 genital defects (?). The use of contrast agents to compensate for the lack of
25 soft-tissue visualization in X-rays can induce complications for patients with

²⁶ renal impairments and allergic reactions (?).

²⁷ Due to its high resolution and large field of view, pre-operative CT is
²⁸ a standard of care for vascular mapping and assessment of intravascular
²⁹ pathology (?). However, CT imaging is typically used for diagnostic and
³⁰ pre-surgical planning, and is limited in it's use for real-time procedural nav-
³¹ igation. CT is also based on ionizing radiation and carries the same risks
³² previously described for fluoroscopy. Furthermore, the surgery cannot be
³³ performed with the patient within the CT bore. In transcatheter proce-
³⁴ dures, there is an unmet need for safe, reliable, radiation-free and real-time
³⁵ image-guidance during vascular navigation.

³⁶ In efforts of minimizing the radiation exposure in Cath labs, near-zero
³⁷ fluoro methods and no-fluoro procedural workflows have also been proposed
³⁸ in the literature (??) to guide the catheters during an ablation procedure
³⁹ and perform transseptal puncture using ICE. Alternative imaging modalities
⁴⁰ such as MR, and US are also considered. Vascular navigation is fundamental
⁴¹ to transcatheter cardiac interventions such as transcatheter aortic valve im-
⁴² plantation (TAVI), caval-valve implantation, and mitral and tricuspid valve
⁴³ annuloplasty, repair and replacement surgeries (?). Accurate representation
⁴⁴ of the vessel geometry is not only important for navigation towards the target
⁴⁵ site, but also for delivering the optimal therapy (??). Procedures such as an-
⁴⁶ gioplasty, stent placement, IVC filter placement all rely on vascular imaging
⁴⁷ to locate the pathological vessel region, select an appropriately sized device,
⁴⁸ and deploy the balloon or stent correctly.

⁴⁹ Catheter-based US technologies such as intravascular US (IVUS) and
⁵⁰ intracardiac echo (ICE) are already indispensable components of Cardiac

51 Catheterization labs (Cath Lab), assisting in the assessment of the disease
52 and device placement. The recent introduction of optical US (OpUS) tech-
53 nology also shows the great potential for the use of catheter-based US for
54 cardiovascular interventions (?). US offers a radiation-free alternative for
55 real-time image guidance. When combined with EM tracking technology, it
56 offers the potential for a large-scale 3D US volume reconstruction, visualiza-
57 tion of anatomy, as well as real-time tool tracking. For most transcatheter
58 interventions, there are two interventional phases - navigation of tools to-
59 wards the target site and positioning of tools to deliver the treatment. In the
60 case of cardiac interventions, vascular navigation is an imperative prerequi-
61 site. Either transfemoral, transradial or transjugular access is required to
62 guide the catheters towards the heart. Inferior vena cava (IVC) navigation,
63 from the groin to the chest, is one of the most common techniques in cardi-
64 ology and is traditionally guided by fluoroscopy. In this paper, the targeted
65 clinical application is the IVC navigation performed during transcatheter
66 cardiovascular interventions.

67 We propose the use of tracked US as an alternative to CT-based vascular
68 mapping and fluoro-guided tool navigation. Instead of using radiation-based
69 imaging to navigate the tools, we propose the following procedural workflow:
70 Prior to the intervention, a tracked, catheter-based US probe (such as ICE,
71 IVUS, or OpUS) scans the desired vasculature and a virtual 3D roadmap is
72 reconstructed. This vascular path can then be easily traversed by a tracked
73 tool or guidewire. This workflow eliminates radiation exposure and the use
74 of heavy lead equipment. Such a system can also be used to make measure-
75 ments of the vessel anatomy and intraluminal buildup. Ultrasound catheters

76 including ICE and IVUS, as well as EM tracking technology are already an
77 indispensable part of a Cath Lab and are used in electrophysiology proce-
78 dures. The proposed ultrasound-based workflow has several advantages over
79 the conventional fluoroscopic techniques. Apart from the lack of radiation,
80 and heavy lead shielding equipment, an US-based navigation system offers
81 full 3D visualization of anatomy, and provides more information to the clin-
82 ician. Furthermore, the use of EM tracking technology allows for tracked
83 tools and catheters which can result in an engaged and informative experi-
84 ence for the clinicians. These features greatly reduce the cognitive load faced
85 by the interventionists and will potentially result in enhanced procedural
86 outcome as well.

87 In this study, we utilized a Foresight ICE system – an intracardiac ul-
88 trasound probe which involves a single-element transducer, spinning on its
89 axis and tilted at a user-specified angle. As a result, the ultrasound image
90 produced is a 2D conical surface image lying in 3D space. One of the biggest
91 advantages of using this probe for navigation is the ‘Forward-viewing’ feature
92 which allows the clinicians to watch where they are going as they traverse
93 the vessels, thus improving their experience and adding a layer of procedural
94 safety. The use of ICE probe is not limited to navigation. For transcatheter
95 cardiac interventions, the ultrasound can further facilitate the delivery of
96 therapy or treatment. This study is geared towards the navigation of inferior
97 vena cava (IVC), it also has the potential to be applied to the navigation
98 of other vessels as well. IVC has many tributaries, but they need not to
99 be navigated for cardiac procedures. The geometry of IVC is also compar-
100 atively simpler than its tributaries like hepatic veins. Since the IVC passes

101 through the entire length of the abdomen, it's surrounding tissues and organs
102 vary along the length. Thus, the appearance of the IVC in the ultrasound
103 varies as well. All these physical and echogenic attributes of IVC are diffi-
104 cult to capture in one phantom. Therefore, for this first, phantom study we
105 are demonstrating the concept on an ultrasound-realistic phantom represent-
106 ing the infrarenal portion of the IVC. The goal is to reconstruct a vascular
107 roadmap without any radiations, safely navigate the guidewire through the
108 vessel, and visualize the guiding catheters as they ascend towards the heart.

109 This paper presents a pilot phantom study as a proof of concept to
110 demonstrate the idea and feasibility of an US-based vascular navigation sys-
111 tem for transcatheter interventions. A vascular phantom was scanned and
112 reconstructed using a forward-looking radial ICE probe and EM tracking
113 technology. The method details, open-source implementation, and phan-
114 tom images are available online for reproducibility (<https://github.com/hareem-nisar/VascularNavigation>). The US-generated vessel model is
115 validated against a CT-scan of the vessel phantom. For a visual validation
116 and concept demonstration of real-time guidance, we also demonstrate nav-
117 igation of a tracked guide-wire in a vascular phantom using the proposed
118 US-based approach.

120 Materials and Methods

121 Data Acquisition

122 A polyvinyl alcohol cryogel (PVA-C) vascular phantom was manufactured
123 to imitate the infra-renal portion of the IVC (?). The phantom generated
124 realistic US imaging when scanned by an intravascular (IVUS) or intracardiac

125 (ICE) US, thus displaying a vessel-mimicking layer, blood-mimicking fluid in
126 the lumen, and a surrounding tissue-mimicking layer. In this study, a 10 Fr,
127 forward-looking, ForesightTM(Conavi Medical Inc., North York, ON, Canada)
128 ICE catheter was used to image the phantom. This probe generates 3D
129 conical surface images, where the angle of the cone is user adjustable. The
130 conical images are projected on a conventional monitor screen as viewed
131 from the apex of the cone and displayed as a circular image. A digital frame-
132 grabber (DVI2USB 3.0, Epiphan Video, Ottawa, ON, Canada) was used
133 to capture the projected ICE images, and the cone-angle information from
134 the console. For US tracking, the ICE probe was rigidly instrumented with
135 a 6DoF pose sensor (Aurora, NDI, Waterloo, ON, Canada) and spatially
136 calibrated using a point-to-line Procrustean approach (??).

137 The vessel phantom was placed in a large water-bath at room-temperature
138 (Fig. 1). The main vessel of the phantom was scanned using the tracked
139 ICE probe at an imaging depth of 80 mm, imaging angle of 67 ° and 12 MHz
140 frequency. Due to some hardware constraints in our set-up, we were only
141 able to scan the central vessel of the phantom and not the branches (details
142 in Discussion section). US images were acquired in real-time using screen-
143 capture. The imaging and tracking data were then processed to reconstruct
144 the surface representation of the vessel from the phantom. The data acquisi-
145 tion, vascular roadmap generation, and the user interface for navigation were
146 all implemented as an open-source software using 3D Slicer (?). The steps
147 involved in the automatic generation of the 3D vascular roadmap include pre-
148 processing to remove image artifacts, lumen segmentation from 2D images
149 and reconstruction of the vessel based on the segmentations and tracking

150 information.

151 *Pre-processing*

152 The acquired screen-captures were cropped to remove any information
153 outside of the US image. The bright reflections in the middle of the cropped
154 US image represent an artifact inherent to the ICE probe (Fig. 2a). This
155 artifact was minimized by using optimal display settings (third level 'wand'
156 function) on the console, and later masking the central bright pixels in the
157 image in our software. The time-gain compensation settings on the console
158 were used to suppress the reflections from the phantom boundary and the
159 container walls. A noise removing filter called the curve flow filter was applied
160 to images to eliminate the interference from by the EM tracker (Fig. 2a) while
161 preserving the contours of the vessel boundary. This was a necessary step
162 prior to performing image processing for lumen segmentation.

163 *Lumen Segmentation*

164 Distinct from imaging using hand-held percutaneous US transducer, the
165 shape of the vessel wall can vary significantly for catheter-based US. Since the
166 US catheters travel through the vasculature adhering close to the vessel wall,
167 the wall does not always appear as a closed circle in the case of radial IVUS
168 and ICE imaging. The first few millimeters of ICE imaging are corrupted by
169 a ring artifact inherent to the radial ICE probe (Fig. 2a). As such, when the
170 ICE catheter is clinging to the vessel wall, the reflection is interrupted close to
171 the center of the image (Fig. 2a) and the vessel boundary appears C-shaped.
172 Therefore, in this study, an edge-based approach was used to segment the
173 vessel lumen from the ICE images, minimizing the error/leakages caused by

174 a discontinuous vessel boundary. A statistics-based active contour algorithm
175 was applied (?). This algorithm grows the boundaries of an initial seed
176 based on the characteristics of the underlying image intensities, and can
177 be manipulated by the parameters ‘intensity homogeneity’ (set to 0.8) and
178 ‘boundary smoothness’ (set to 1) to maintain the roundness of the contour
179 and minimize leakages based on intensity.

180 The performance of the segmentation algorithm is highly dependent on
181 the size and placement of the initial seed. Therefore, for the algorithm to be
182 effective, it is necessary to have an initial seed, closely fitted to and completely
183 encapsulated and centered within the vessel lumen (?). The Hough transform
184 was used to approximate the initial seed by fitting a circle to the lumen (Fig.
185 2b) (Parameters values: Hough Gradient, dp =1, min_dist=100, param1=95,
186 param2=20). Gaussian blur was applied prior to the Hough transform to
187 avoid over-detection of circles. To ensure that the seed does not overlap
188 with the vessel boundary, the fitted circle was iteratively decreased in radius
189 until there were no bright reflections in the underlying image. A hundred
190 and eighty image frames were processed and 2D lumen segmentations were
191 acquired for each image.

192 *Vessel Reconstruction*

193 The ForesightTMICE probe generates forward-looking conical surface im-
194 ages. The images acquired by this device, and subsequently the lumen seg-
195 mentation, were a version of the true US data projected onto a 2D disk. 2D
196 lumen segmentations were subjected to 3D conversion to reconstruct true,
197 conical segmentations (Fig. 2c) using the radius and imaging angle informa-
198 tion, available through the console. This reconstruction is governed by the

199 equation:

$$\begin{bmatrix} x_{3D} \\ y_{3D} \\ z_{3D} \end{bmatrix} = \begin{bmatrix} 1 & 0 & -o_x \\ 0 & 1 & -o_y \\ 0 & 0 & \|(x_{2D}), y_{2D})\| \cdot \tan(90 - \phi) \end{bmatrix} \begin{bmatrix} x_{2D} \\ y_{2D} \\ 1 \end{bmatrix} \quad (1)$$

200 where (o_x, o_y) represents the center of the planar image or the apex of the
201 conical image, and ϕ represents the imaging angle of the cone-shaped im-
202 age. Each segmentation was positioned and scaled to its correct shape and
203 location in 3D space by applying US probe calibration and tracking infor-
204 mation, producing a skeleton of the vessel (Fig. 3a). The vessel skeleton
205 was then processed to form a closed 3D surface representation using binary
206 morphological closing, with an annulus kernel of size [60, 60] to fill the gaps
207 between consecutive segments. For final smoothing of the reconstructed ves-
208 sel, a Gaussian blur with a standard deviation of 3 was applied. The result
209 represents the 3D model of the vessel scanned from our phantom (Fig. 3b),
210 spatially present in the EM tracker's coordinate system.

211 *Validation*

212 As described previously, vascular navigation is currently achieved using
213 fluoroscopy or CT mapping. The vessel phantom was imaged using US, and
214 the vessel was reconstructed and compared with X-ray and CT. Geometric
215 accuracy of the US reconstructed vessel model was validated against the
216 vessel segmented from the CT scan of the same phantom. The absolute
217 surface-to-surface distance between the two models were computed after a
218 rigid registration (?). For vascular navigation, one of the clinically relevant
219 goals is to know the overall alignment of the vessels in space. To evaluate

220 the spatial alignment, we used DICE metrics which compares the spatial
 221 overlap between the reconstructed and CT vessel after CT-US registration
 222 was performed. False positive spatial region in the reconstructed US vessel is
 223 also an important metric and must be minimal to avoid the misrepresentation
 224 of the vessel. For many vascular procedures, the clinical objective is to
 225 avoid puncturing the vessels. In such cases, the boundary accuracy becomes
 226 important as well as the false positive regions. To evaluate the contours of the
 227 reconstructed vessel, we calculated the Hausdorff distance (HD) metrics (?).
 228 Volumetric analysis was not performed as volume-based metrics are invariant
 229 of segmentation shape and boundary and thus can be misleading. As a
 230 visual validation, we demonstrate what US-based navigation may look like.
 231 A tracked, straight-tip guidewire(?), augmented with a 5DOF EM sensor,
 232 was maneuvered to navigate the vessels in the phantom.

233 **Results**

234 The absolute distance between the US reconstrcuted vessel and the reg-
 235 istered CT segmenetd vessel was computed and presented as a heatmap on
 236 the vessel surface in Fig. 3c. The average distance between the surface of
 237 the two models comes out to be 1.7 ± 1.12 mm. A maximum error of 5.86 mm
 238 between the two surface models was observed. The spatial overlap between
 239 the registered US and CT models was evaluated using the Dice coefficient,
 240 sensitivity and specificity measures where

$$Dice = \frac{\text{True positive overlap between CT and US vessels}}{(\text{num voxels CTvessel}) * (\text{num voxels USvessel})} \quad (2)$$

241 The spatial distance between the two model boundaries was evaluated
242 using the Hausdorff distance (HD). The geometric accuracy results are re-
243 ported in Table 1. Comparison showed that the US model had 12.93 % false
244 negative and 6.60 % false positive spatial overlap.

245 The x-ray imaging of our phantom, along with a guidewire, is represented
246 in Fig. 4a. In comparison, we can also achieve tool guidance using an US-
247 guided vascular navigation system. Fig. 4b shows how the US reconstructed
248 vessel looks like in 3D space. Virtual representation of a tracked guidewire
249 can be seen in context, as it navigates the phantom vessel.

250 **Discussion**

251 In this study, we present an vascular reconstruction-based navigation sys-
252 tem, which provides a safe and radiation-free method for guiding tools during
253 transcatheter procedures. An EM-tracked ICE US probe was used to recon-
254 struct the vascular path in a phantom, such that it can be visualized in a
255 common coordinate system with a tracked guidewire for vessel navigation.
256 The results indicate that the average error in terms of HD is 1.7 mm, with a
257 3.16 mm confidence interval, which is a clinically acceptable value (?). During
258 navigation, it is important to identify the vessel boundary and the regions
259 outside the vessel lumen so as to not puncture or damage the vessel wall.
260 Our results indicate that only 6.60 % region lies outside the ground truth
261 provided by the CT scan of the phantom. This over-segmentation is due to
262 the leakages through the discontinuous wall boundary in some of the images
263 when the ultrasound probe is clinging to the vessel wall. The accuracy of the
264 navigation system can further be improved by improving the segmentation

265 and tracking accuracy as discussed below.

266 The resulting error is a combination of many different errors in the sys-
267 tem, such as EM tracking inaccuracies, propagation of calibration errors, US
268 probe hardware constraints, registration errors, and relative motion of the
269 phantom if any. One of the major limitations of our study is defined by the
270 sensorizing the US probe and its calibration accuracy. This inaccuracy can
271 be minimized by applying a manual offset correction for the imaging angle.
272 The ICE probe used in this study has a small diameter of 3.3 mm which re-
273 quired rigidly fixing the sensor on the outer sheath of the probe, farther away
274 from the origin of the image. The rigid and outer positioning of sensor led
275 to some hardware constraints resulting in our inability to turn and guide the
276 probe into the branches of the vessel. This limitation is strictly a character-
277 istic of our experimental setup in this preliminary study using a Foresight™
278 ICE probe. The proposed idea can be extended to other radial ultrasound
279 catheters as well. Ideally the tracking sensor should be integrated within
280 the US catheter and pre-calibrated by the manufacturers to eliminate any
281 limitation of maneuvering the US. For a clinical system, the EM sensor must
282 be integrated inside the US catheter to achieve accuracy in tracking, free-
283 dom in motion and patient safety from an active element. In the future, we
284 plan to collaborate with the ICE probe manufacturers to acquire ICE probes
285 embedded with EM sensors and designing a prototype of the US guidance
286 system presented as a concept study in this paper.

287 The proposed US-based vascular navigation system can be implemented
288 using many catheter-based US technology, such as radial IVUS probes that
289 are regularly used during cardiac and endovascular interventions. Other than

tracking, the accuracy of a clinical vessel reconstruction algorithm will also largely depend on the accuracy of lumen segmentation from in-vivo imaging. The appearance of a vessel in an intravascular or intracardiac US image varies significantly depending on the size and composition of the vessel, as well as the surrounding tissue and organs. The phantom images presented in this study replicate the US imaging of the infrarenal portion of IVC only. Even the echogenicity of the IVC changes as it passes through the abdomen. Thus a clinical system, implementing the proposed idea of US navigation, will require a robust deep learning-based segmentation pipeline, which is capable of accurately identifying and segmenting all vascular structures as well as vessel branches and tributaries. Existing network architectures, such as U-Net, might be a suitable option for medical image segmentation. Since this is a pilot, proof of concept study for navigation with relatively restricted imaging data, we did not include any learning based approaches for segmentation and relied on conventional image processing techniques.

In future work we aim to improve this vascular reconstruction pipeline by replacing the image-processing based vessel segmentation algorithm with a deep learning-based segmentation technique trained on animal images acquired using the forward-looking, Foresight™ICE probe. The use of machine-learning for vascular segmentation and reconstruction has been previously performed using both surface US scans (??) and intravascular US (?). The integration of a machine-learning based segmentation will allow for accurate patient specific reconstructions to be obtained that account for differences in patients pathology. The segmentation algorithm can be trivially replaced within our vascular reconstruction pipeline such that the different vessels

315 required for navigation can be reconstructed using a robust segmentation al-
316 gorithm capable of delineating various vascular morphologies and side vessel
317 branches, allowing for safe navigation from the insertion site to the central
318 venous system.

319 The phantom based workflow presented in this paper is time consuming
320 due to the computationally expensive vessel segmentation technique used.
321 For clinical purposes, the vessel segmentation step should be fast and robust.
322 However, this is a first proof of concept study and the vessel segmentation
323 step is only suitable for the phantom images. Therefore, to replace the cur-
324 rent vessel segmentation step, we have developed a real-time segmentation
325 technique for isolating vessel lumina from ultrasound imaging of inferior vena
326 cava in animals.¹ We are also currently working towards optimizing the
327 presented pipeline to perform the vessel reconstruction in order of seconds.
328 Combining the optimized reconstruction algorithm with the real-time vessel
329 segmentation method will enable a time-apt image guidance system ready
330 for pre-clinical studies.

331 The accuracy of the vessel reconstruction algorithm presented in this
332 paper largely depends on the accuracy of the vessel segmentation and the
333 tracking technology used. The electromagnetic tracking has submillimeter
334 accuracy, however the vessel segmentation does not. As mentioned earlier,
335 we have developed a real-time vessel segmentation method using deep learn-
336 ing. This new segmentation method relies on a trained U-net model to accu-
337 rately segment the complex-shaped vessel lumina from the ICE imaging of the

¹The preprint has been made available at research gate (DOI: 10.13140/RG.2.2.31644.82567)

338 vena cava from a swine. This deep learning based method is robust against
339 boundary artifacts such as intraluminal buildups and stents. However, the
340 algorithm produce inaccurate segmentation when a lead is present inside the
341 vessel. Any artifacts outside the vessel and present in the surrounding tissue
342 do not have a significant impact on the accuracy of our vessel segmentation
343 and reconstruction. To cater for the any artefacts, the new segmentation
344 technique can be trivially modified without disturbing the entire reconstruc-
345 tion pipeline presented in this paper. Deep learning based systems benefit
346 from a variety of imaging datasets in making the segmentation algorithm
347 more robust. By retraining the U-net model on different examples of vascu-
348 lar imaging with artifacts, the segmentation and thus the reconstruction can
349 be made robust and accurate.

350 Another limitation is the size of the US catheter. The US probe used in
351 this study is a 10 Fr device which is large and less suitable for the arterial
352 system, although it is usually not problematic for venous interventions. This
353 is a limitation of the current technology (Foresight™ ICE probe by Conavi
354 Medical Inc.) and ideally this device will be miniaturized by the manufactur-
355 ers in the near future. The workflow presented in this paper can potentially
356 be adapted for intravascular ultrasound (IVUS) imaging where the catheter is
357 much smaller. For example, the Novasight Hybrid (by Conavi Medical Inc.)
358 is a combined IVUS-OCT imaging catheter with a size of 3.3 French (?).

359 **Conclusions**

360 Transcatheter interventions provide a low-impact means of delivering
361 therapy using miniaturized equipment and medical imaging technologies.

362 Vascular navigation is a ubiquitous process as it is a prerequisite to reach the
363 target organ or target site in another vessel. The current standard of care
364 employs fluoroscopic techniques or the use of CT vascular mapping, both
365 of which come at a cost of radiation exposure and wearing heavy, shielding
366 aprons. Through this study, we aim to initiate a discussion on the merits
367 of moving towards the use of ultrasound-based instead of radiation-based
368 techniques for transcatheter and endovascular interventions. We present a
369 proof of concept study to use catheter-based US technology, equipped with
370 tracking sensors, to create a vascular roadmap. Results indicate that the
371 geometric accuracy is comparable to that observed in CT mapping. The
372 concept demonstration (Fig. 4) shows side by side that an US-guided system
373 can provide the same level of information and in three dimensions without
374 the hazards of radiation and lead shielding.

375 **Acknowledgements**

376 The authors would like to thank Dr. Dan Bainbridge (London Health
377 Sciences Centre) and John Moore (Archetype Biomedical Inc.) for their
378 valuable discussion and insight into the project. We acknowledge our sources
379 of funding - Canadian Institutes of Health Research (CIHR) and Candaian
380 Foundation for Innovation (CFI). The grants are held by Dr. Terry Peters.
381 The authors would also like to thank Conavi Medical Inc. for providing the
382 ultrasound imaging dataset.

383 **Figure Captions**

384 **Figure 1:** Data acquisition setup - Ultrasound probe scans the vessel phan-
385 tom present within the tracking space.

386 **Figure 2:** (a) Image data acquired using a framegrabber as a 2D projec-
387 tion of the conical ultrasound. (b) Lumen segmentation (boundary)
388 achieved using the initial seed (solid). (c) Conical reconstruction of the
389 ultrasound image and the lumen segmentation.

390 **Figure 3:** Image a) depicts the skeleton of the vessel comprised of spatially
391 calibrated segmentations, Image b) depicts the ultrasound (US) re-
392 construction registered to the segmented CT scan of the phantom, and
393 Image c) provides a visualization of the surface-to-surface distance anal-
394 ysis between the US and CT models.

395 **Figure 4:** An example use case for navigating a tracked guidewire within the
396 ultrasound reconstructed vessel (b) as compared to the fluoroscopic
397 equivalent (a)

398 **Tables**

399 **Table 1:** Summary of the metrics use to quantify The spatial overlap and
400 boundary accuracy of the ultrasound reconstructed vessel compared to
401 the vessel segmented from the CT scan of the phantom.

Spatial Overlap	Value	Hausdorff Distance (mm)	Value
DICE Coefficient	0.79	Maximum	5.86
Sensitivity	0.70	Average	1.63
Specificity	0.88	95 %	3.16

Towards fluoro-free interventions: Using radial intracardiac ultrasound for vascular navigation

Hareem Nisar^{a,b,*}, Leah Groves^{a,b}, Leandro Cardarelli-Leite^c, Terry M. Peters^{a,b,d}, Elvis C.S. Chen^{a,b,d}

^a*Robarts Research Institute, Western University, London, ON, Canada*

^b*Department of Biomedical Engineering, Western University, London, ON, Canada*

^c*London Health Sciences Centre, London, ON, Canada*

^d*Department of Medical Biophysics, Western University, London, ON, Canada*

Abstract

Transcatheter cardiovascular interventions have the advantage of patient safety, reduced surgery time, and minimal trauma to the patient's body. Transcathether interventions, which are performed percutaneously are limited by the lack of direct line-of-sight with the procedural tools and the patient anatomy. Therefore, such interventional procedures rely heavily on image guidance for navigating towards and delivering therapy at the target site. Vascular navigation via the inferior vena cava (IVC), from the groin to the heart, is an imperative part of most transcatheter cardiovascular interventions including heart valve repair surgeries and ablation therapy. Traditionally, the IVC is navigated using fluoroscopic techniques such as venography or CT venography. These X-ray based techniques can have detrimental effects on the patient as well as the surgical team, causing increased radiation exposure, leading to risk of cancer, fetal defects, and eye

*Corresponding Author: Hareem Nisar, Robarts Research Institute, 1151 Richmond St. N. London, ON N6A 5B7; Email, hnисar3@uwo.ca; Phone, 519.931.5777

cataracts. The use of heavy lead apron has also been reported to cause back pain and spine issues thus leading to interventionalist's disc disease. We propose the use of a catheter-based ultrasound augmented with electromagnetic (EM) tracking technology to generate a vascular roadmap in real-time and perform navigation without harmful radiation. In this pilot study, we use spatially-tracked intracardiac echocardiography (ICE) to reconstruct a vessel from a phantom in a 3D virtual environment. We demonstrate how the proposed ultrasound-based navigation will appear in a virtual environment, by navigating a tracked guidewire within the vessels in the phantom without any radiation-based imaging. The geometric accuracy is assessed using a CT scan of the phantom, with a Dice coefficient of 0.79. The average distance between the surface of the two models comes out to be 1.7 ± 1.12 mm.

Keywords: Transcatheter interventions, Vascular navigation, Fluoro-free, Transfemoral guidance, Vascular Disease

1 Introduction

2 Advances in medical imaging, combined with miniaturized and flexible
3 procedural tools, have allowed surgical procedures to be performed percu-
4 taneously using transcatheter-based approaches. These minimally invasive
5 approaches have increased patient safety, decreased procedure time, and low-
6 ered complication rates (Jahangiri et al., 2019). Catheter-directed therapies
7 inherently prohibits the direct line-of-sight with the anatomy and the tools.
8 Interventionalists rely heavily on image-guidance to navigate and position
9 their tools to deliver therapy at the target region. Common imaging modal-
10 ities used for transcatheter-based interventions include X-ray fluoroscopy,
11 computed tomography (CT), magnetic resonance imaging (MRI), and in-
12 travascular (IVUS), intracardiac (ICE) or transesophageal (TEE) ultrasound
13 (US).

14 Fluoroscopy is commonly used for minimally invasive procedures as it pro-
15 vides real-time, high contrast vascular images, by means of X-ray imaging
16 with contrast enhancement. The radiation exposure produced by X-rays can
17 be harmful to the patient, clinical staff, and medical trainees, even when used
18 in conjunction with various shielding techniques (Theocharopoulos et al.,
19 2006; Christopoulos et al., 2016). The use of heavy shielding aprons may have
20 detrimental effects on the physical health of the interventional team causing
21 "interventionalist's disc disease" (Ross et al., 1997) which includes back and
22 neck pain (Dixon et al., 2017), cervical disc herniation, and other spinal and
23 musculoskeletal issues (Goldstein et al., 2004), as well as the possibility of
24 lead poisoning (Katsari et al., 2020). Interventional cardiologists and radiol-
25 ogists have reported developing eye cataracts (Jacob et al., 2013), increased

26 risk of cancer (Roguin et al., 2013), and increased risk of fetal congenital
27 defects (Limacher et al., 1998). The use of contrast agents to compensate
28 for the lack of soft-tissue visualization in X-rays can induce complications
29 for patients with renal impairments and allergic reactions (Davenport et al.,
30 2015).

31 Due to its high resolution and large field of view, pre-operative CT is
32 a standard of care for vascular mapping and assessment of intravascular
33 pathology (Murphy et al., 2018). However, CT imaging is typically used for
34 diagnostic and pre-surgical planning, and is limited in it's use for real-time
35 procedural navigation. CT is also based on ionizing radiation and carries the
36 same risks previously described for fluoroscopy. Furthermore, the surgery
37 cannot be performed with the patient within the CT bore. In transcatheter
38 procedures, there is an unmet need for safe, reliable, radiation-free and real-
39 time image-guidance during vascular navigation.

40 In efforts of minimizing the radiation exposure in Cath labs, near-zero
41 fluoro methods and no-fluoro procedural workflows have also been proposed
42 in the literature (Stec et al., 2014; Zhang et al., 2020) to guide the catheters
43 during an ablation procedure and perform transseptal puncture using ICE.
44 Alternative imaging modalities such as MR, and US are also considered.
45 Vascular navigation is fundamental to transcatheter cardiac interventions
46 such as transcatheter aortic valve implantation (TAVI), caval-valve implan-
47 tation, and mitral and tricuspid valve annuloplasty, repair and replacement
48 surgeries (Prendergast et al., 2019). Accurate representation of the vessel
49 geometry is not only important for navigation towards the target site, but
50 also for delivering the optimal therapy (Murphy et al., 2017; Shammas et al.,

51 2019). Procedures such as angioplasty, stent placement, IVC filter placement
52 all rely on vascular imaging to locate the pathological vessel region, select an
53 appropriately sized device, and deploy the balloon or stent correctly.

54 Catheter-based US technologies such as intravascular US (IVUS) and
55 intracardiac echo (ICE) are already indispensable components of Cardiac
56 Catheterization labs (Cath Lab), assisting in the assessment of the disease
57 and device placement. The recent introduction of optical US (OpUS) tech-
58 nology also shows the great potential for the use of catheter-based US for
59 cardiovascular interventions (Little et al., 2020). US offers a radiation-free
60 alternative for real-time image guidance. When combined with EM tracking
61 technology, it offers the potential for a large-scale 3D US volume recon-
62 struction, visualization of anatomy, as well as real-time tool tracking. For
63 most transcatheter interventions, there are two interventional phases - nav-
64 igation of tools towards the target site and positioning of tools to deliver
65 the treatment. In the case of cardiac interventions, vascular navigation is
66 an imperative prerequisite. Either transfemoral, transradial or transjugular
67 access is required to guide the catheters towards the heart. Inferior vena
68 cava (IVC) navigation, from the groin to the chest, is one of the most com-
69 mon techniques in cardiology and is traditionally guided by fluoroscopy. In
70 this paper, the targeted clinical application is the IVC navigation performed
71 during transcatheter cardiovascular interventions.

72 We propose the use of tracked US as an alternative to CT-based vascular
73 mapping and fluoro-guided tool navigation. Instead of using radiation-based
74 imaging to navigate the tools, we propose the following procedural workflow:
75 Prior to the intervention, a tracked, catheter-based US probe (such as ICE,

76 IVUS, or OpUS) scans the desired vasculature and a virtual 3D roadmap is
77 reconstructed. This vascular path can then be easily traversed by a tracked
78 tool or guidewire. This workflow eliminates radiation exposure and the use
79 of heavy lead equipment. Such a system can also be used to make measure-
80 ments of the vessel anatomy and intraluminal buildup. Ultrasound catheters
81 including ICE and IVUS, as well as EM tracking technology are already an
82 indispensable part of a Cath Lab and are used in electrophysiology proce-
83 dures. The proposed ultrasound-based workflow has several advantages over
84 the conventional fluoroscopic techniques. Apart from the lack of radiation,
85 and heavy lead shielding equipment, an US-based navigation system offers
86 full 3D visualization of anatomy, and provides more information to the clin-
87 ician. Furthermore, the use of EM tracking technology allows for tracked
88 tools and catheters which can result in an engaged and informative experi-
89 ence for the clinicians. These features greatly reduce the cognitive load faced
90 by the interventionalists and will potentially result in enhanced procedural
91 outcome as well.

92 In this study, we utilized a Foresight ICE system – an intracardiac ul-
93 trasound probe which involves a single-element transducer, spinning on its
94 axis and tilted at a user-specified angle. As a result, the ultrasound image
95 produced is a 2D conical surface image lying in 3D space. One of the biggest
96 advantages of using this probe for navigation is the ‘Forward-viewing’ feature
97 which allows the clinicians to watch where they are going as they traverse
98 the vessels, thus improving their experience and adding a layer of procedural
99 safety. The use of ICE probe is not limited to navigation. For transcatheter
100 cardiac interventions, the ultrasound can further facilitate the delivery of

101 therapy or treatment. This study is geared towards the navigation of inferior
102 vena cava (IVC), it also has the potential to be applied to the navigation
103 of other vessels as well. IVC has many tributaries, but they need not to
104 be navigated for cardiac procedures. The geometry of IVC is also compar-
105 atively simpler than its tributaries like hepatic veins. Since the IVC passes
106 through the entire length of the abdomen, it's surrounding tissues and organs
107 vary along the length. Thus, the appearance of the IVC in the ultrasound
108 varies as well. All these physical and echogenic attributes of IVC are diffi-
109 cult to capture in one phantom. Therefore, for this first, phantom study we
110 are demonstrating the concept on an ultrasound-realistic phantom represent-
111 ing the infrarenal portion of the IVC. The goal is to reconstruct a vascular
112 roadmap without any radiations, safely navigate the guidewire through the
113 vessel, and visualize the guiding catheters as they ascend towards the heart.

114 This paper presents a pilot phantom study as a proof of concept to
115 demonstrate the idea and feasibility of an US-based vascular navigation sys-
116 tem for transcatheter interventions. A vascular phantom was scanned and
117 reconstructed using a forward-looking radial ICE probe and EM tracking
118 technology. The method details, open-source implementation, and phan-
119 tom images are available online for reproducibility (<https://github.com/hareem-nisar/VascularNavigation>). The US-generated vessel model is
120 validated against a CT-scan of the vessel phantom. For a visual validation
121 and concept demonstration of real-time guidance, we also demonstrate nav-
122 igation of a tracked guide-wire in a vascular phantom using the proposed
123 US-based approach.

125 **Materials and Methods**

126 *Data Acquisition*

127 A polyvinyl alcohol cryogel (PVA-C) vascular phantom was manufactured
128 to imitate the infra-renal portion of the IVC (Nisar et al., 2020). The phan-
129 tom generated realistic US imaging when scanned by an intravascular (IVUS)
130 or intracardiac (ICE) US, thus displaying a vessel-mimicking layer, blood-
131 mimicking fluid in the lumen, and a surrounding tissue-mimicking layer. In
132 this study, a 10 Fr, forward-looking, Foresight™(Conavi Medical Inc., North
133 York, ON, Canada) ICE catheter was used to image the phantom. This
134 probe generates 3D conical surface images, where the angle of the cone is
135 user adjustable. The conical images are projected on a conventional monitor
136 screen as viewed from the apex of the cone and displayed as a circular im-
137 age. A digital frame-grabber (DVI2USB 3.0, Epiphan Video, Ottawa, ON,
138 Canada) was used to capture the projected ICE images, and the cone-angle
139 information from the console. For US tracking, the ICE probe was rigidly in-
140 strumented with a 6DoF pose sensor (Aurora, NDI, Waterloo, ON, Canada)
141 and spatially calibrated using a point-to-line Procrustean approach (Chen
142 et al., 2016; Nisar et al., 2019).

143 The vessel phantom was placed in a large water-bath at room-temperature
144 (Fig. 1). The main vessel of the phantom was scanned using the tracked
145 ICE probe at an imaging depth of 80 mm, imaging angle of 67 ° and 12 MHz
146 frequency. Due to some hardware constraints in our set-up, we were only
147 able to scan the central vessel of the phantom and not the branches (details
148 in Discussion section). US images were acquired in real-time using screen-
149 capture. The imaging and tracking data were then processed to reconstruct

150 the surface representation of the vessel from the phantom. The data acqui-
151 sition, vascular roadmap generation, and the user interface for navigation
152 were all implemented as an open-source software using 3D Slicer (Fedorov
153 et al., 2012). The steps involved in the automatic generation of the 3D
154 vascular roadmap include pre-processing to remove image artifacts, lumen
155 segmentation from 2D images and reconstruction of the vessel based on the
156 segmentations and tracking information.

157 *Pre-processing*

158 The acquired screen-captures were cropped to remove any information
159 outside of the US image. The bright reflections in the middle of the cropped
160 US image represent an artifact inherent to the ICE probe (Fig. 2a). This
161 artifact was minimized by using optimal display settings (third level 'wand'
162 function) on the console, and later masking the central bright pixels in the
163 image in our software. The time-gain compensation settings on the console
164 were used to suppress the reflections from the phantom boundary and the
165 container walls. A noise removing filter called the curve flow filter was applied
166 to images to eliminate the interference from by the EM tracker (Fig. 2a) while
167 preserving the contours of the vessel boundary. This was a necessary step
168 prior to performing image processing for lumen segmentation.

169 *Lumen Segmentation*

170 Distinct from imaging using hand-held percutaneous US transducer, the
171 shape of the vessel wall can vary significantly for catheter-based US. Since the
172 US catheters travel through the vasculature adhering close to the vessel wall,
173 the wall does not always appear as a closed circle in the case of radial IVUS

and ICE imaging. The first few millimeters of ICE imaging are corrupted by a ring artifact inherent to the radial ICE probe (Fig. 2a). As such, when the ICE catheter is clinging to the vessel wall, the reflection is interrupted close to the center of the image (Fig. 2a) and the vessel boundary appears C-shaped. Therefore, in this study, an edge-based approach was used to segment the vessel lumen from the ICE images, minimizing the error/leakages caused by a discontinuous vessel boundary. A statistics-based active contour algorithm was applied (Gao et al., 2010). This algorithm grows the boundaries of an initial seed based on the characteristics of the underlying image intensities, and can be manipulated by the parameters ‘intensity homogeneity’ (set to 0.8) and ‘boundary smoothness’ (set to 1) to maintain the roundness of the contour and minimize leakages based on intensity.

The performance of the segmentation algorithm is highly dependent on the size and placement of the initial seed. Therefore, for the algorithm to be effective, it is necessary to have an initial seed, closely fitted to and completely encapsulated and centered within the vessel lumen (Gao et al., 2010). The Hough transform was used to approximate the initial seed by fitting a circle to the lumen (Fig. 2b) (Parameters values: Hough Gradient, $dp = 1$, $\text{min_dist} = 100$, $\text{param1} = 95$, $\text{param2} = 20$). Gaussian blur was applied prior to the Hough transform to avoid over-detection of circles. To ensure that the seed does not overlap with the vessel boundary, the fitted circle was iteratively decreased in radius until there were no bright reflections in the underlying image. A hundred and eighty image frames were processed and 2D lumen segmentations were acquired for each image.

198 *Vessel Reconstruction*

199 The Foresight™ICE probe generates forward-looking conical surface im-
 200 ages. The images acquired by this device, and subsequently the lumen seg-
 201 mentation, were a version of the true US data projected onto a 2D disk. 2D
 202 lumen segmentations were subjected to 3D conversion to reconstruct true,
 203 conical segmentations (Fig. 2c) using the radius and imaging angle informa-
 204 tion, available through the console. This reconstruction is governed by the
 205 equation:

$$\begin{bmatrix} x_{3D} \\ y_{3D} \\ z_{3D} \end{bmatrix} = \begin{bmatrix} 1 & 0 & -o_x \\ 0 & 1 & -o_y \\ 0 & 0 & \|(x_{2D}, y_{2D})\| \cdot \tan(90 - \phi) \end{bmatrix} \begin{bmatrix} x_{2D} \\ y_{2D} \\ 1 \end{bmatrix} \quad (1)$$

206 where (o_x, o_y) represents the center of the planar image or the apex of the
 207 conical image, and ϕ represents the imaging angle of the cone-shaped im-
 208 age. Each segmentation was positioned and scaled to its correct shape and
 209 location in 3D space by applying US probe calibration and tracking infor-
 210 mation, producing a skeleton of the vessel (Fig. 3a). The vessel skeleton
 211 was then processed to form a closed 3D surface representation using binary
 212 morphological closing, with an annulus kernel of size [60, 60] to fill the gaps
 213 between consecutive segments. For final smoothing of the reconstructed ves-
 214 sel, a Gaussian blur with a standard deviation of 3 was applied. The result
 215 represents the 3D model of the vessel scanned from our phantom (Fig. 3b),
 216 spatially present in the EM tracker's coordinate system.

217 *Validation*

218 As described previously, vascular navigation is currently achieved using
219 fluoroscopy or CT mapping. The vessel phantom was imaged using US, and
220 the vessel was reconstructed and compared with X-ray and CT. Geomet-
221 ric accuracy of the US reconstructed vessel model was validated against the
222 vessel segmented from the CT scan of the same phantom. The absolute
223 surface-to-surface distance between the two models were computed after a
224 rigid registration (Besl and McKay, 1992). For vascular navigation, one of
225 the clinically relevant goals is to know the overall alignment of the vessels
226 in space. To evaluate the spatial alignment, we used DICE metrics which
227 compares the spatial overlap between the reconstructed and CT vessel af-
228 ter CT-US registration was performed. False positive spatial region in the
229 reconstructed US vessel is also an important metric and must be minimal
230 to avoid the misrepresentation of the vessel. For many vascular procedures,
231 the clinical objective is to avoid puncturing the vessels. In such cases, the
232 boundary accuracy becomes important as well as the false positive regions.
233 To evaluate the contours of the reconstructed vessel, we calculated the Haus-
234 dorff distance (HD) metrics (Taha and Hanbury, 2015). Volumetric analysis
235 was not performed as volume-based metrics are invariant of segmentation
236 shape and boundary and thus can be misleading. As a visual validation, we
237 demonstrate what US-based navigation may look like. A tracked, straight-
238 tip guidewire(Piazza et al., 2020), augmented with a 5DOF EM sensor, was
239 maneuvered to navigate the vessels in the phantom.

240 **Results**

241 The absolute distance between the US reconstructed vessel and the reg-
242 istered CT segmented vessel was computed and presented as a heatmap on
243 the vessel surface in Fig. 3c. The average distance between the surface of
244 the two models comes out to be 1.7 ± 1.12 mm. A maximum error of 5.86 mm
245 between the two surface models was observed. The spatial overlap between
246 the registered US and CT models was evaluated using the Dice coefficient,
247 sensitivity and specificity measures where

$$Dice = \frac{\text{True positive overlap between CT and US vessels}}{(\text{num voxels CTvessel}) * (\text{num voxels USvessel})} \quad (2)$$

248 The spatial distance between the two model boundaries was evaluated
249 using the Hausdorff distance (HD). The geometric accuracy results are re-
250 ported in Table 1. Comparison showed that the US model had 12.93 % false
251 negative and 6.60 % false positive spatial overlap.

252 The x-ray imaging of our phantom, along with a guidewire, is represented
253 in Fig. 4a. In comparison, we can also achieve tool guidance using an US-
254 guided vascular navigation system. Fig. 4b shows how the US reconstructed
255 vessel looks like in 3D space. Virtual representation of a tracked guidewire
256 can be seen in context, as it navigates the phantom vessel.

257 **Discussion**

258 In this study, we present an vascular reconstruction-based navigation
259 system, which provides a safe and radiation-free method for guiding tools
260 during transcatheter procedures. An EM-tracked ICE US probe was used

261 to reconstruct the vascular path in a phantom, such that it can be visu-
262 alized in a common coordinate system with a tracked guidewire for vessel
263 navigation. The results indicate that the average error in terms of HD is
264 1.7 mm, with a 3.16 mm confidence interval, which is a clinically acceptable
265 value (Linte et al., 2012). During navigation, it is important to identify
266 the vessel boundary and the regions outside the vessel lumen so as to not
267 puncture or damage the vessel wall. Our results indicate that only 6.60 %
268 region lies outside the ground truth provided by the CT scan of the phantom.
269 This over-segmentation is due to the leakages through the discontinuous wall
270 boundary in some of the images when the ultrasound probe is clinging to the
271 vessel wall. The accuracy of the navigation system can further be improved
272 by improving the segmentation and tracking accuracy as discussed below.

273 The resulting error is a combination of many different errors in the sys-
274 tem, such as EM tracking inaccuracies, propagation of calibration errors, US
275 probe hardware constraints, registration errors, and relative motion of the
276 phantom if any. One of the major limitations of our study is defined by the
277 sensorizing the US probe and its calibration accuracy. This inaccuracy can
278 be minimized by applying a manual offset correction for the imaging angle.
279 The ICE probe used in this study has a small diameter of 3.3 mm which re-
280 quired rigidly fixing the sensor on the outer sheath of the probe, farther away
281 from the origin of the image. The rigid and outer positioning of sensor led
282 to some hardware constraints resulting in our inability to turn and guide the
283 probe into the branches of the vessel. This limitation is strictly a character-
284 istic of our experimental setup in this preliminary study using a Foresight™
285 ICE probe. The proposed idea can be extended to other radial ultrasound

286 catheters as well. Ideally the tracking sensor should be integrated within
287 the US catheter and pre-calibrated by the manufacturers to eliminate any
288 limitation of maneuvering the US. For a clinical system, the EM sensor must
289 be integrated inside the US catheter to achieve accuracy in tracking, free-
290 dom in motion and patient safety from an active element. In the future, we
291 plan to collaborate with the ICE probe manufacturers to acquire ICE probes
292 embedded with EM sensors and designing a prototype of the US guidance
293 system presented as a concept study in this paper.

294 The proposed US-based vascular navigation system can be implemented
295 using many catheter-based US technology, such as radial IVUS probes that
296 are regularly used during cardiac and endovascular interventions. Other than
297 tracking, the accuracy of a clinical vessel reconstruction algorithm will also
298 largely depend on the accuracy of lumen segmentation from in-vivo imaging.
299 The appearance of a vessel in an intravascular or intracardiac US image varies
300 significantly depending on the size and composition of the vessel, as well as
301 the surrounding tissue and organs. The phantom images presented in this
302 study replicate the US imaging of the infrarenal portion of IVC only. Even
303 the echogenicity of the IVC changes as it passes through the abdomen. Thus
304 a clinical system, implementing the proposed idea of US navigation, will re-
305 quire a robust deep learning-based segmentation pipeline, which is capable of
306 accurately identifying and segmenting all vascular structures as well as ves-
307 sel branches and tributaries. Existing network architectures, such as U-Net,
308 might be a suitable option for medical image segmentation. Since this is a
309 pilot, proof of concept study for navigation with relatively restricted imaging
310 data, we did not include any learning based approaches for segmentation and

311 relied on conventional image processing techniques.

312 In future work we aim to improve this vascular reconstruction pipeline
313 by replacing the image-processing based vessel segmentation algorithm with
314 a deep learning-based segmentation technique trained on animal images ac-
315 quired using the forward-looking, Foresight™ICE probe. The use of machine-
316 learning for vascular segmentation and reconstruction has been previously
317 performed using both surface US scans (Groves et al., 2020; Yang et al.,
318 2013) and intravascular US (Yang et al., 2018). The integration of a machine-
319 learning based segmentation will allow for accurate patient specific recon-
320 structions to be obtained that account for differences in patients pathology.
321 The segmentation algorithm can be trivially replaced within our vascular re-
322 construction pipeline such that the different vessels required for navigation
323 can be reconstructed using a robust segmentation algorithm capable of de-
324 lineating various vascular morphologies and side vessel branches, allowing for
325 safe navigation from the insertion site to the central venous system.

326 The phantom based workflow presented in this paper is time consuming
327 due to the computationally expensive vessel segmentation technique used.
328 For clinical purposes, the vessel segmentation step should be fast and robust.
329 However, this is a first proof of concept study and the vessel segmentation
330 step is only suitable for the phantom images. Therefore, to replace the cur-
331 rent vessel segmentation step, we have developed a real-time segmentation
332 technique for isolating vessel lumina from ultrasound imaging of inferior vena
333 cava in animals. ¹. We are also currently working towards optimizing the

¹The preprint has been made available at research gate (DOI: 10.13140/RG.2.2.31644.82567)

334 presented pipeline to perform the vessel reconstruction in order of seconds.
335 Combining the optimized reconstruction algorithm with the real-time vessel
336 segmentation method will enable a time-apt image guidance system ready
337 for pre-clinical studies.

338 The accuracy of the vessel reconstruction algorithm presented in this
339 paper largely depends on the accuracy of the vessel segmentation and the
340 tracking technology used. The electromagnetic tracking has submillimeter
341 accuracy, however the vessel segmentation does not. As mentioned earlier,
342 we have developed a real-time vessel segmentation method using deep learn-
343 ing. This new segmentation method relies on a trained U-net model to accu-
344 rately segment the complex-shaped vessel lumina from the ICE imaging of the
345 vena cava from a swine. This deep learning based method is robust against
346 boundary artifacts such as intraluminal buildups and stents. However, the
347 algorithm produce inaccurate segmentation when a lead is present inside the
348 vessel. Any artifacts outside the vessel and present in the surrounding tissue
349 do not have a significant impact on the accuracy of our vessel segmentation
350 and reconstruction. To cater for the any artefacts, the new segmentation
351 technique can be trivially modified without disturbing the entire reconstruc-
352 tion pipeline presented in this paper. Deep learning based systems benefit
353 from a variety of imaging datasets in making the segmentation algorithm
354 more robust. By retraining the U-net model on different examples of vascu-
355 lar imaging with artifacts, the segmentation and thus the reconstruction can
356 be made robust and accurate.

357 Another limitation is the size of the US catheter. The US probe used in
358 this study is a 10 Fr device which is large and less suitable for the arterial

359 system, although it is usually not problematic for venous interventions. This
360 is a limitation of the current technology (Foresight™ ICE probe by Conavi
361 Medical Inc.) and ideally this device will be miniaturized by the manufactur-
362 ers in the near future. The workflow presented in this paper can potentially
363 be adapted for intravascular ultrasound (IVUS) imaging where the catheter is
364 much smaller. For example, the Novasight Hybrid (by Conavi Medical Inc.)
365 is a combined IVUS-OCT imaging catheter with a size of 3.3 French (Ono
366 et al., 2020).

367 **Conclusions**

368 Transcatheter interventions provide a low-impact means of delivering
369 therapy using miniaturized equipment and medical imaging technologies.
370 Vascular navigation is a ubiquitous process as it is a prerequisite to reach the
371 target organ or target site in another vessel. The current standard of care
372 employs fluoroscopic techniques or the use of CT vascular mapping, both
373 of which come at a cost of radiation exposure and wearing heavy, shielding
374 aprons. Through this study, we aim to initiate a discussion on the merits
375 of moving towards the use of ultrasound-based instead of radiation-based
376 techniques for transcatheter and endovascular interventions. We present a
377 proof of concept study to use catheter-based US technology, equipped with
378 tracking sensors, to create a vascular roadmap. Results indicate that the
379 geometric accuracy is comparable to that observed in CT mapping. The
380 concept demonstration (Fig. 4) shows side by side that an US-guided system
381 can provide the same level of information and in three dimensions without
382 the hazards of radiation and lead shielding.

383 Acknowledgements

384 The authors would like to thank Dr. Dan Bainbridge (London Health
385 Sciences Centre) and John Moore (Archetype Biomedical Inc.) for their
386 valuable discussion and insight into the project. We acknowledge our sources
387 of funding - Canadian Institutes of Health Research (CIHR) and Candaian
388 Foundation for Innovation (CFI). The grants are held by Dr. Terry Peters.
389 The authors would also like to thank Conavi Medical Inc. for providing the
390 ultrasound imaging dataset.

391 **References**

- 392 Besl P, McKay ND. A method for registration of 3-d shapes. IEEE Transactions on Pattern Analysis and Machine Intelligence, 1992;14:239–256.
- 393
- 394 Chen ECS, Peters TM, Ma B. Guided ultrasound calibration: where, how, and how many calibration fiducials. International Journal of Computer Assisted Radiology and Surgery, 2016;11:889–898.
- 395
- 396
- 397 Christopoulos G, Makke L, Christakopoulos G, Kotsia A, Rangan BV, Roesle M, Haagen D, Kumbhani DJ, Chambers CE, Kapadia S, Mahmud E, Banerjee S, Brilakis ES. Optimizing Radiation Safety in the Cardiac Catheterization Laboratory. Catheterization and Cardiovascular Interventions, 2016;87:291–301.
- 398
- 399
- 400
- 401
- 402 Davenport MS, Cohan RH, Ellis JH. Contrast Media Controversies in 2015: Imaging Patients With Renal Impairment or Risk of Contrast Reaction. American Journal of Roentgenology, 2015;204:1174–1181.
- 403
- 404
- 405 Dixon RG, Khiatani V, Statler JD, Walser EM, Midia M, Miller DL, Bartal G, Collins JD, Gross KA, Stecker MS, Nikolic B. Society of Interventional Radiology: Occupational Back and Neck Pain and the Interventional Radiologist. Journal of Vascular and Interventional Radiology, 2017;28:195–199.
- 406
- 407
- 408
- 409 Fedorov A, Beichel R, Kalpathy-Cramer J, Finet J, Fillion-Robin JC, Pu-jol S, Bauer C, Jennings D, Fennessy F, Sonka M, Buatti J, Aylward S, Miller JV, Pieper S, Kikinis R. 3D Slicer as an image computing platform for the Quantitative Imaging Network. Magnetic resonance imaging, 2012;30:1323–41.
- 410
- 411
- 412
- 413

- ⁴¹⁴ Gao Y, Tannenbaum A, Kikinis R. Simultaneous multi-object segmentation using local robust statistics and contour interaction. In: International
⁴¹⁵ MICCAI Workshop on Medical Computer Vision. Springer, 2010. pp. 195–
⁴¹⁶ 203.
- ⁴¹⁷
- ⁴¹⁸ Goldstein JA, Balter S, Cowley M, Hodgson J, Klein LW. Occupational hazards of interventional cardiologists: Prevalence of orthopedic health problems in contemporary practice. *Catheterization and Cardiovascular Interventions*, 2004;63:407–411.
- ⁴¹⁹
- ⁴²⁰
- ⁴²¹
- ⁴²² Groves LA, VanBerlo B, Veinberg N, Alboog A, Peters TM, Chen EC. Automatic segmentation of the carotid artery and internal jugular vein from
⁴²³ 2d ultrasound images for 3d vascular reconstruction. *International journal of computer assisted radiology and surgery*, 2020.
- ⁴²⁴
- ⁴²⁵
- ⁴²⁶ Jacob S, Boveda S, Bar O, Brézin A, Maccia C, Laurier D, Bernier MO. Interventional cardiologists and risk of radiation-induced cataract: Results
⁴²⁷ of a French multicenter observational study. *International Journal of Cardiology*, 2013;167:1843–1847.
- ⁴²⁸
- ⁴²⁹
- ⁴³⁰ Jahangiri M, Hussain A, Akowuah E. Minimally invasive surgical aortic valve
⁴³¹ replacement. *Heart*, 2019;105:s10–s15.
- ⁴³²
- ⁴³³
- ⁴³⁴
- ⁴³⁵ Katsari K, Paraskevopoulou C, Barati M, Kostopoulou E, Griskevicius R, Blazquez N, Tekin HO, Illing RO. Lead exposure in clinical imaging—the elephant in the room. *European Journal of Radiology*, 2020;131:109210.
- ⁴³⁶
- ⁴³⁷ Limacher MC, Douglas PS, Germano G, Laskey WK, Lindsay BD, Mcketty MH, Moore ME, Park JK, Prigent FM, Walsh MN, Forrester JS, Faxon

- 437 DP, Fisher JD, Gibbons RJ, Halperin JL, Hutter AM, Kaul S, Skorton DJ,
438 Weintraub WS, Winters WL, Wolk MJ. Radiation Safety in the Practice
439 of Cardiology. Tech. rep., 1998.
- 440 Linet CA, Lang P, Rettmann ME, Cho DS, Holmes DR, Robb RA, Peters
441 TM. Accuracy Considerations in Image-guided Cardiac Interventions: Ex-
442 perience and Lessons Learned. International journal of computer assisted
443 radiology and surgery, 2012;7:13.
- 444 Little CD, Colchester RJ, Noimark S, Manmathan G, Finlay MC, Desjardins
445 AE, Rakhit RD. Optically generated ultrasound for intracoronary imaging.
446 Frontiers in Cardiovascular Medicine, 2020;7.
- 447 Murphy DJ, Aghayev A, Steigner ML. Vascular CT and MRI: a practical
448 guide to imaging protocols. Insights into Imaging, 2018;9:215–236.
- 449 Murphy EA, Ross RA, Jones RG, Gandy SJ, Aristokleous N, Salsano M,
450 Weir-McCall JR, Matthew S, Houston JG. Imaging in Vascular Access.
451 Cardiovascular Engineering and Technology, 2017;8:255–272.
- 452 Nisar H, Moore J, Alves-Kotzev N, Hwang GYS, Peters TM, Chen ECS.
453 Ultrasound calibration for unique 2.5D conical images. In: Fei B, Linet
454 CA (Eds.), Medical Imaging 2019: Image-Guided Procedures, Robotic
455 Interventions, and Modeling. SPIE, 2019. p. 78.
- 456 Nisar H, Moore J, Piazza R, Maneas E, Chen ECS, Peters TM. A sim-
457 ple, realistic walled phantom for intravascular and intracardiac applica-
458 tions. International Journal of Computer Assisted Radiology and Surgery,
459 2020;15:1513–1523.

- ⁴⁶⁰ Ono M, Kawashima H, Hara H, Gao C, Wang R, Kogame N, Takahashi K,
⁴⁶¹ Chichareon P, Modolo R, Tomaniak M, Wykrzykowska JJ, Piek JJ, Mori
⁴⁶² I, Courtney BK, Wijns W, Sharif F, Bourantas C, Onuma Y, Serruys
⁴⁶³ PW. Advances in IVUS/OCT and Future Clinical Perspective of Novel
⁴⁶⁴ Hybrid Catheter System in Coronary Imaging. *Frontiers in Cardiovascular*
⁴⁶⁵ *Medicine*, 2020;7:119.
- ⁴⁶⁶ Piazza R, Nisar H, Moore J, Condino S, Ferrari M, Ferrari V, Peters T,
⁴⁶⁷ Chen E. Towards electromagnetic tracking of J-tip guidewire: precision
⁴⁶⁸ assessment of sensors during bending tests. In: Fei B, Linte CA (Eds.),
⁴⁶⁹ *Medical Imaging 2020: Image-Guided Procedures, Robotic Interventions,*
⁴⁷⁰ and Modeling. SPIE, 2020. p. 5.
- ⁴⁷¹ Prendergast BD, Baumgartner H, Delgado V, Gérard O, Haude M, Him-
⁴⁷² melmann A, Iung B, Leafstedt M, Lennartz J, Maisano F, Marinelli EA,
⁴⁷³ Modine T, Mueller M, Redwood SR, Rörick O, Sahyoun C, Saillant E,
⁴⁷⁴ Søndergaard L, Thoenes M, Thomitzek K, Tschernich M, Vahanian A,
⁴⁷⁵ Wendler O, Zemke EJ, Bax JJ. Transcatheter heart valve interventions:
⁴⁷⁶ where are we? Where are we going? *European Heart Journal*, 2019;40:422–
⁴⁷⁷ 440.
- ⁴⁷⁸ Roguin A, Goldstein J, Bar O, Goldstein JA. Brain and Neck Tumors Among
⁴⁷⁹ Physicians Performing Interventional Procedures. *The American Journal*
⁴⁸⁰ *of Cardiology*, 2013;111:1368–1372.
- ⁴⁸¹ Ross AM, Segal J, Borenstein D, Jenkins E, Cho S. Prevalence of Spinal
⁴⁸² Disc Disease Among Interventional Cardiologists. *The American Journal*
⁴⁸³ *of Cardiology*, 1997;79:68–70.

- 484 Shammas N, Radaideh Q, Shammas WJ, Daher GE, Rachwan RJ, Radaideh
485 Y. The role of precise imaging with intravascular ultrasound in coro-
486 nary and peripheral interventions. Vascular Health and Risk Management,
487 2019;Volume 15:283–290.
- 488 Stec S, Śledz J, Mazij M, Ras M, Ludwik B, Chrabaszcz M, Śledz A, Ba-
489 nasik M, Bzymek M, Mlynarczyk K, Deutsch K, Labus M, Śpikowski J,
490 Szydłowski L. Feasibility of Implementation of a “Simplified, No-X-Ray,
491 No-Lead Apron, Two-Catheter Approach” for Ablation of Supraventricu-
492 lar Arrhythmias in Children and Adults. Journal of Cardiovascular Elec-
493 trophysiology, 2014;25:866–874.
- 494 Taha AA, Hanbury A. Metrics for evaluating 3D medical image segmentation:
495 analysis, selection, and tool. BMC Medical Imaging, 2015;15:29.
- 496 Theocharopoulos N, Damilakis J, Perisinakis K, Manios E, Vardas P, Gourt-
497 soyiannis N. Occupational exposure in the electrophysiology laboratory:
498 quantifying and minimizing radiation burden. The British Journal of Ra-
499 diology, 2006;79:644–651.
- 500 Yang J, Tong L, Faraji M, Basu A. Ivus-net: an intravascular ultrasound
501 segmentation network. In: International Conference on Smart Multimedia.
502 Springer, 2018. pp. 367–377.
- 503 Yang X, Jin J, Xu M, Wu H, He W, Yuchi M, Ding M. Ultrasound common
504 carotid artery segmentation based on active shape model. Computational
505 and mathematical methods in medicine, 2013;345968.

506 Zhang G, Cheng L, Liang Z, Zhang J, Dong R, Hang F, Wang X,
507 Wang Z, Zhao L, Wang Z, Wu Y. Zero-fluoroscopy transseptal puncture
508 guided by right atrial electroanatomical mapping combined with intrac-
509 ardiac echocardiography: A single-center experience. Clinical Cardiology,
510 2020;43:1009–1016.

511 **Figure Captions**

512 **Figure 1:** Data acquisition setup - Ultrasound probe scans the vessel phan-
513 tom present within the tracking space.

514 **Figure 2:** (a) Image data acquired using a framegrabber as a 2D projec-
515 tion of the conical ultrasound. (b) Lumen segmentation (boundary)
516 achieved using the initial seed (solid). (c) Conical reconstruction of the
517 ultrasound image and the lumen segmentation.

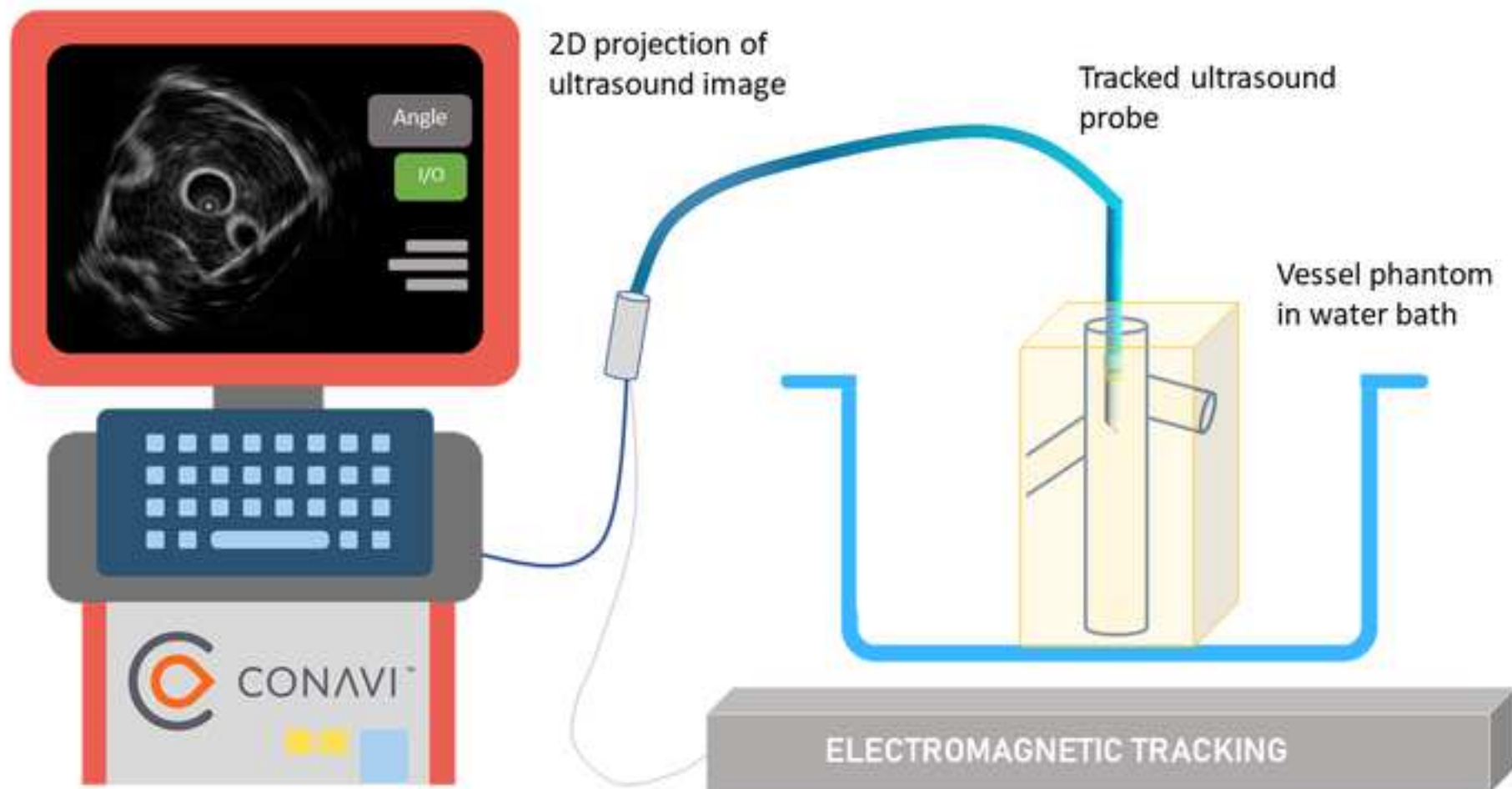
518 **Figure 3:** Image a) depicts the skeleton of the vessel comprised of spatially
519 calibrated segmentations, Image b) depicts the ultrasound (US) re-
520 construction registered to the segmented CT scan of the phantom, and
521 Image c) provides a visualization of the surface-to-surface distance anal-
522 ysis between the US and CT models.

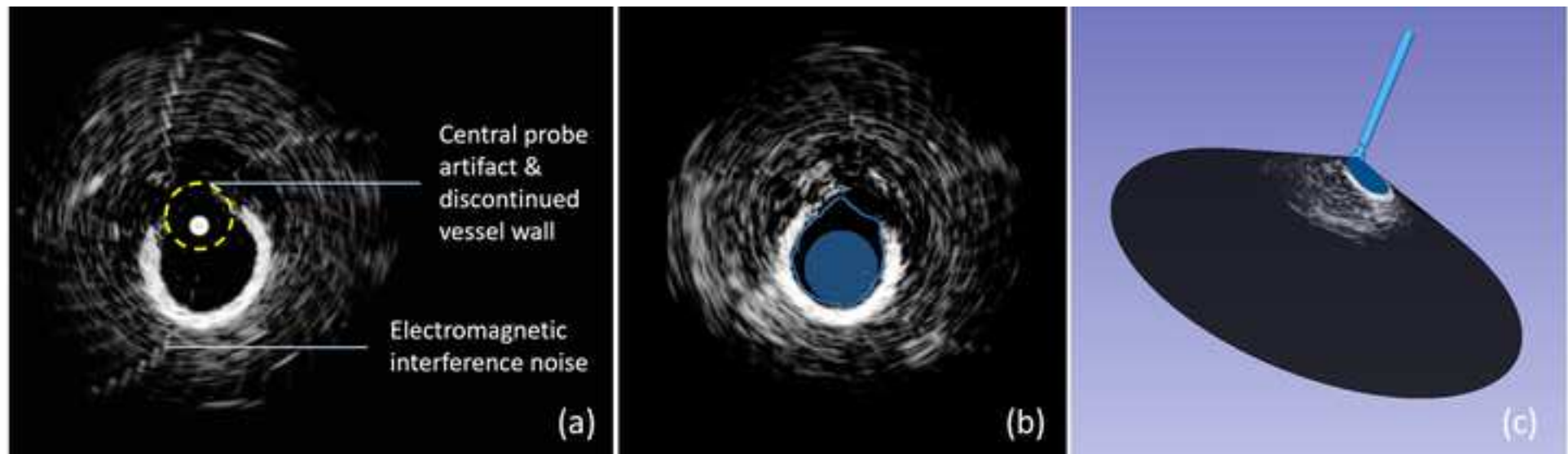
523 **Figure 4:** An example use case for navigating a tracked guidewire within the
524 ultrasound reconstructed vessel (b) as compared to the fluoroscopic
525 equivalent (a)

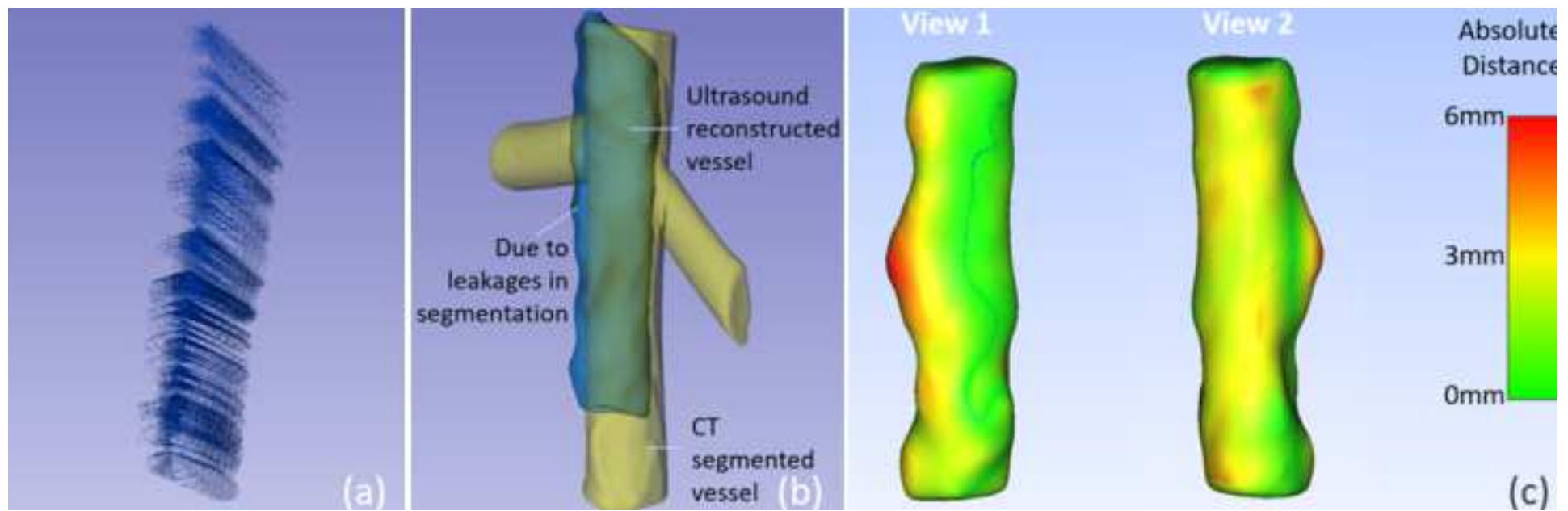
526 **Tables**

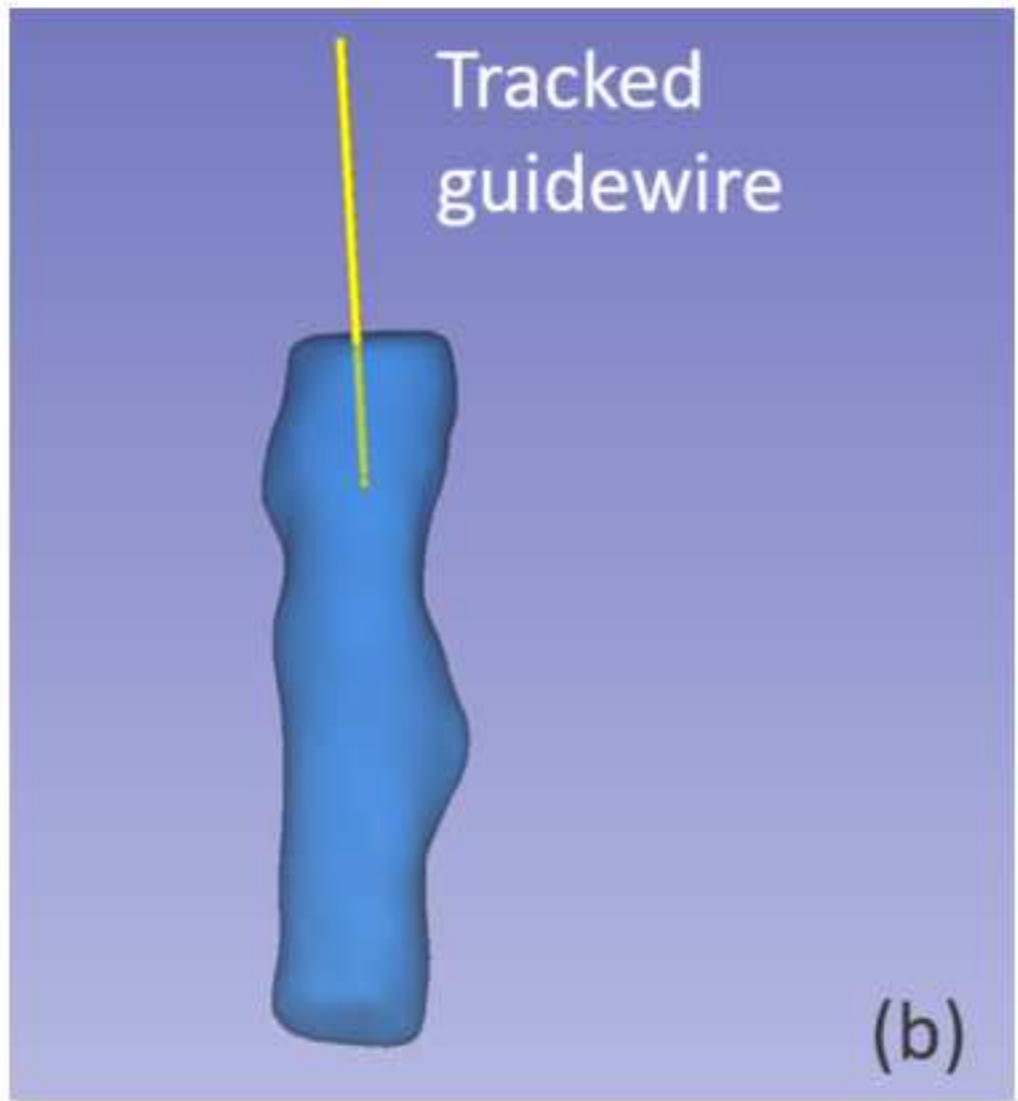
527 **Table 1:** Summary of the metrics use to quantify The spatial overlap and
528 boundary accuracy of the ultrasound reconstructed vessel compared to
529 the vessel segmented from the CT scan of the phantom.

Spatial Overlap	Value	Hausdorff Distance (mm)	Value
DICE Coefficient	0.79	Maximum	5.86
Sensitivity	0.70	Average	1.63
Specificity	0.88	95 %	3.16











Click here to access/download
LaTeX Source Files
elsarticle.cls



Click here to access/download
LaTeX Source Files
UMB-elsarticle-harvbib.bst



Click here to access/download

LaTeX Source Files
UMB-elsarticle-template-harv.tex



Click here to access/download
LaTeX Source Files
UMB2021BIB.bib